Green Synthesis of Mono and Bimetallic Nanoparticles of Silver and Cobalt Oxide Using *Croton Macrostaychus* Plant Extract and Evaluation of their Antibacterial Activity

Fikadu Worku Alemu

A Thesis Submitted to Department of Applied Chemistry

School of Applied Natural Science

Presented in Partial Fulfillment of the Requirements for the Master of Science Degree in Applied Chemistry (Inorganic chemistry)

Office of Postgraduate Studies

Adama Science and Technology University

November, 2022

Adama, Ethiopia

Green Synthesis of Mono and Bimetallic Nanoparticles of Silver and Cobalt Oxide Using *Croton Macrostaychus* Plant Extract and evaluation of their Antibacterial Activity

Fikadu Worku Alemu

Advisor: Tegene Desalegn (Ph.D.)

A Thesis Submitted to Department of Applied Chemistry,
School of Applied Natural Science
Presented in Partial Fulfillment of the Requirements for the Master of Science Degree in Applied Chemsitry (Inorganic chemistry)

Office of Postgraduate Studies
Adama Science and Technology University

November, 2022
Adama, Ethiopia

Declaration

I hereby declare that the MSc Thesis report entitled "**Green Synthesis of Mono and Bimetallic Nanoparticles of Silver and Cobalt Oxide Using *Croton Macrostaychus* Plant Extract and Evaluation of their Antibacterial Activity"** is my original work and has not been presented for a degree in any other university and all sources of material used for this thesis have been duly acknowledged.

Fikadu Worku Alemu _____ _____

Name of the Student Signature Date

Recommendation

I, the advisor of this thesis, hereby certify that we have read the revised version of the thesis entitled "**Green Synthesis of Mono and Bimetallic Nanoparticles of Silver and Cobalt Oxide Using *Croton Macrostaychus* Plant Extract and Evaluation of their Antibacterial Activity"** prepared under our guidance to **Fikadu Worku Alemu** submitted in partial fulfillment of the requirements for the degree of Master of Science in Inorganic chemistry. Therefore, I recommend the submission of the revised version of the thesis to the department following the applicable procedures.

_____	_____	_____
Advisor	Signature	Date

Approval Page

I, the advisor of the thesis entitled "**Green Synthesis of Mono and Bimetallic Nanoparticles of Silver and Cobalt Oxide Using *Croton Macrostaychus* Plant Extract and Evaluation of their Antibacterial Activity"** and developed by **Fikadu Worku Alemu**, hereby certify that the recommendation and suggestions made by the board of examiners are appropriately incorporated into the final version of the thesis.

_____	_____	_____
Advisor	Signature	Date

We, the undersigned, members of the Board of Examiners of the thesis by **Fikadu Worku Alemu** have read and evaluated the thesis entitled "**Green Synthesis of Mono and Bimetallic Nanoparticles of Silver and Cobalt Oxide Using *Croton Macrostaychus* Plant Extract and Evaluation of their Antibacterial Activity"** and examined the candidate during the open defense. This is, therefore, to certify that the thesis is accepted for partial fulfillment of the requirement of the degree of Master of Science in Applied Chemistry (Inorganic chemistry).

_____	_____	_____
Chairperson	Signature	Date
_____	_____	_____
Internal Examiner	Signature	Date
_____	_____	_____
External Examiner	Signature	Date

Finally, approval and acceptance of the thesis is contingent upon submission of its final copy to the Office of Postgraduate Studies (OPGS) through the Department Graduate Council (DGC) and School Graduate Committee (SGC).

_____	_____	_____
Department Head	Signature	Date
_____	_____	_____
School Dean	Signature	Date
_____	_____	_____
Office of Postgraduate Studies,	Signature	Date

ACKNOWLEDGEMENT

First of all, I thank Almighty God for being with me in all aspects of my work. He has always been with me, led my path and helped me to achieve my goals.

Conducting this thesis research could not be fruitful without the generous help of individuals. In particular, I would like to express my sincere and heartfelt gratitude to my advisor Dr. Tegene Desalegn who helped me with continuous guidance and encouragement in all aspects of this work. Next, I would to thank Bule Hora University, Colleague of Natural and Computational Science Department of Chemistry for giving me Scholar ship opportunity. And also I would like to give my thanks to Adama Science and Technology University, the School of Applied Natural Science, department of Applied Chemistry for facilitation of all laboratory works.

I would also like to thank the Department of Applied Biology for allowing me to use Scanning Electron Microscopy, the Department of Materials Science Engineering for allowing me to use XRD instruments, and Addis Ababa Science and technology University College of Natural Science for running UV-Vis Spectroscopy, Bahirdar University for running FTIR analysis, Adama public health referrals and research laboratory center conduct Antibacterial Activity Applications.

My thanks also extend to my families, friends and colleagues for their encouragement, help and comments given in proceeding of my work

TABLE OF CONTENTS

CONTENTS **PAGE**

LIST OF TABLES

LIST OF FIGURES

LIST OF ABBREVATION

Ag NPs	Silver nanoparticles
Ag/Co_3O_4 NPs	Silver-Cobalt oxide nanoparticles
Au-Ag NPs	Gold- Silver nanoparticles
BMNPs	Bimetallic nanoparticles
Co NPs	Cobalt nanoparticles
Cu NPs	Copper nanoparticles
DMF	Dimethylformamide
DMSO	Dimethyl sulfoxide
EDX	Energy-dispersive X-ray
FT-IR	Fourier Transmission Infrared Spectroscopy
HRTEM	High-resolution transmission electron microscopy
MNPs	Metal nanoparticles
MMNPs	Monometallic nanoparticles
MONPs	Metal oxide nanoparticles
NMs	Nanomaterials
NPs	Nanoparticles
NSMs	Nanostructured materials
SAED	Selected Area Electron Diffraction
SEM	Scanning electron microscopy
SPR	Surface palsmon resonance
TEM	Transmission electron microscopy
TGA	Thermal gravimetric analysis
XRD	X-ray Diffractometry

LIST OF ACCRONOMYS

AMR	Antimicrobial resistance
ATCC	American Type Culture Collection
DNA	Deoxyribonucleic acid
EPA	Environmental Protection Agency
EU	European Union
ISO	International Organization for Standardization
MRSA	Methicillin-resistant Staphylococcus aureus
NADH	Nicotinamide adenine dinucleotide hydrogen
USA	United States of America
USFDA	United states Food and Drug Administration
UV-VIS	Ultraviolet-Visible spectroscopy
VRSA	Vancomycin-resistant Staphylococcus aureus
WHO	World Health Organization
AMR	Antimicrobial resistance

ABSTRACT

In this study, Ag NPs, Co_3O_4 NPs and Ag/Co_3O_4 BMNPs were synthesized via the green synthesis method by using Croton macrostachyus leaf extract. The synthesized NPs were characterized by using spectroscopic techniques such as X-ray diffraction (XRD), scanning electron microscopy (SEM), Fourier Transform Infrared (FT-IR) and UV-Vis spectroscopy. The XRD results confirmed cubic crystal structure for the Ag NPs with an average crystallite size of 12.62 nm and cubic spinel crystal structure for Co_3O_4 NPs having an average crystallite size of 12.746 nm and also the average crystal size of Ag/ Co_3O_4 BMNPs was found to be 18.07 nm. From the UV-Vis (DRS) data result, the energy band gap of Ag NPs, Co_3O_4 NPs and Ag/Co_3O_4 BMNPs were found to be 3.38 eV, 3.34 eV and 3.54 eV respectively. The SEM images showed clusters or large nanoparticles for Ag NPs and spherical as well as irregular geometries which was associated with non-homogeneity of the particles in terms of their shape and size for Co_3O_4 NPs and Ag/Co_3O_4 BMNPs. The FT-IR to identify the bioactive molecules which were actively involved during the synthesis process as stabilizing and capping agents to prevent the overall growth of Ag NPs, Co_3O_4NPs and Ag/Co_3O_4 BMNPs. The antibacterial activities of the synthesized nanoparticles were tested against gram-negative bacterial strains (Escherichia-coli, Salmonella typhimrium), and gram-positive strains (Staphylococcus aureus and Enterococcus faecalis) using the agar-well diffusion method. Ag/Co_3O_4 BMNPs exhibited best inhibition activities toward the selected bacterial species (Escherichia-coli and Staphylococcus aureus) than that of Ag NPs and Co_3O_4NPs inhibition activities. However, Ag NPs exhibited best inhibition activities toward Salmonella typhimrium and Enterococcus faecalis bacteria species. Co_3O_4 NPs showed least inhibition activities against selected bacterial species compared to Ag NPs and Ag/Co_3O_4 BMNPs.

Key words: *Ag NPs, Co_3O_4 NPs, bimetallic nanoparticles, Green synthesis, Croton macrostachyus plant, Antibacterial activity.*

1. INTRODUCTION

1.1. Back ground

For several years antimicrobial resistance (AMR) has been a growing threat to the effective treatment of an ever-increasing range of infectious diseases caused by bacteria, parasites, viruses and fungi. AMR results in reduced efficiency of antibacterial, antiparasitic, antiviral and antifungal drugs, making the treatment of patients difficult, costly, or even impossible. The impact on particularly vulnerable patients is most obvious, resulting in prolonged illness and increased mortality (World Health Organization, 2014). The severity and widespread nature of antibiotic resistance result in limited treatments to efficiently combat antibiotic-resistant pathogens (Davies & Davies, 2010; Magiorakos et al., 2012). Most of antibiotics that are currently in use have three bacterial targets: the cell wall synthesis, translational machinery, and DNA replication machinery. Inappropriately, bacterial resistance can develop against each of these modes of action. Therefore, the development of new drugs is needed. One possible concept of drug improvement is effect enhancement by means of nanoparticles, thus allowing the binding of metals, proteins, phospholipids and antibodies (Crisan et al., 2021).

Due to an exceptional antibacterial performance and high specific surface area, nanomaterials are the most promising antimicrobial substances, and bacteria can hardly develop resistance due to the complex antibacterial mechanism of nanomaterials. Most of the antibiotic resistance mechanisms are irrelevant for nanoparticles (NPs) because the mode of action of NPs is direct contact with the bacterial cell wall, without the need to penetrate the cell; this increases the confidence that NPs would be less prone to encouraging resistance in bacteria than antibiotics. Therefore, attention has been focused on new and exciting NP-based materials with antibacterial activity (Wang et al., 2017; Guo et al., 2020).

Nanoparticles can be defined as at least one of their dimensions must fall below 100 nm. However, the most interesting properties related to nanoparticles are best revealed for dimensions below 10 nm. Such particles exhibit high surface-to-volume ratios. In recent years, BMNPs are well known and gained great importance and interest with their enhanced optical, electrical, and catalytic properties compared to the single component nanoparticles (NPs) due to their composition and synergistic effects (Dsouza et al., 2021; Herlekar et al., 2014; Shafey, 2020).

Bimetallic Nanoparticles (BMNPs) can be defined as the combination of two metals in the nanoscale size range that exhibit numerous new and improved properties. Monometallic nanoparticles obtain the property of their constituent metal while bimetallic and trimetallic alloy nanoparticles synthesized from two or three metals show more stable structures and enhanced properties. Therefore, bimetallic nanoparticles are being progressively studied for potentially diverse applications (Huynh et al., 2020; Prechtl & Campbell, 2013). Various metallic and bimetallic oxides have been synthesized by many researchers; for instance, manganese-zinc oxide (Prasankumar et al., 2017), copper-cereum oxide (Zhu et al., 2008), tin-manganese oxide (Chiang et al., 2014), palladium-copper oxide (Yuan et al., 2014), palladium-gold (Ksar et al., 2009), iron- copper oxide (Y. Wang et al., 2015), Manganese-Tin Oxide (Khan et al., 2019) and palladium-nickel oxide (Zhang et al., 2016) etc. These bimetallic oxides show multiple functionalities and prominent activity, selectivity and stability which attributes to their unique lattice structure and synergistic interaction.

A number of chemical, physical and biological approaches are currently employed for the fabrication of nanoparticles. Biological based synthesis using plants and their extracts, enzymes and microbes is considered as the most ecofriendly alternative to physical and chemical methods. Using plant-based synthesis methods are beneficial over other biological procedures as they eliminate the complex process of cell culture maintenance. Plant contain a considerable number of both capping and reducing agents, such as flavonoids, polyphenols, and other reducing components, which can reduce salts to zero-valent and avoid agglomeration (Alvi et al., 2021).

Many studies have been reported on biological synthesis of either Co or Ag nanoparticles. In contrast, much lesser work has been done or reported on the biological synthesis of Ag-Co bimetallic nanoparticles. In case of monometallic Silver NPs (Ag NPs) are known to be the most effective against bacteria and viruses and also Cobalt NPs also have an intrinsic advantage in biomedical related fields, e.g., drug delivery and magnetic resonance imaging (Ansari et al., 2017). However, the study on antibacterial effects of copper nanoparticles using *E. coli* and *Bacillus subtilis* revealed that the Cu NPs exhibited superior antibacterial activity compared to the silver nanoparticles. This indicates antibacterial activity of silver NPs is less when compared to Copper nanoparticle in case of monometallic NPs (Crisan et al., 2021). But, silver based bimetallic nanoparticle shows high bacterial efficiency to the pathogenic bacteria

(Padilla-Cruz et al., 2021). Therefore, the present work presents the Green Synthesis of Mono and Bimetallic Nanoparticles of Silver and Cobalt Oxide Using *Croton Macrostaychus* Plant Extract and evaluation of their Antibacterial Activity.

The Croton *macrostachyus* is one of the most abundant plants in some African countries including Eritrea, Ethiopia, Kenya, Tanzania and Uganda. It belongs to the genus *Croton L.*, *Euphorbiaceae* family, called Croton under the sub family *Crotonoideae*, which comprises more than 1200 species of herbs, shrubs, trees, and occasionally lianas. The genus Croton is used in traditionally for the treatment of several human health problems including diabetes, malaria, dysentery, stomachache, and ascariasis in different areas. Croton *macrostachyus* contains numerous bioactive compounds such as alkaloids, amino acids, anthraquinones, carbohydrates, cardiac glycosides, coumarins, essential oil, fatty acids, flavonoids, phenolic compounds, phlobatannins, polyphenols, phytosteroides, saponins, sterols, tannins, terpenoids, unsaturated sterol and vitamin C have been identified from *C. macrostachyus* fruits, leaves, stem bark, and twigs (Letha et al 2016; Obey et al 2018; Gebrehiwota et al., 2018). These components are critical to the formation of metal nanoparticles. They are also biodegradable, environmentally safe, and can act as capping and reducing agents. Therefore, the plant parts employed for the green synthesis of NPs, instead of using toxic and too costly capping and reducing agents.

1.2. Statement of the problem

Microbial infectious disease are becoming among the major threat to public health, which increase mortality rates and costs in hospitals, with the fast spread of drug-resistant infectious diseases constituting a global threat to human health. The severity and widespread nature of antibiotic resistance result in limited treatments to efficiently combat antibiotic-resistant pathogens. Nanoparticles have different or enhanced properties in contrast to their bulk material, including antimicrobial efficiency towards a broad range of microorganisms. In addition to this, Nanoparticles and nanomaterials are products of a quickly growing technology. They are widely applied in many fields; catalysis, electronics, biology and biomedical material science, cosmetics, renewable energies, physics and environmental remediation due to their distinctive properties. Unfortunately, use of toxic organic solvents and strong reducing agents during nanoparticles synthesis has posed great risk to the environment.

Hence, the development of eco-friendly and cheap nanomaterials is a necessity. In this study, the utilization of *Croton macrostachyus* plant extracts in biosynthesis of Ag NPs, Co_3O_4 NPs and Ag/Co_3O_4 BMNPs have been studied including the antibacterial activity of Ag NPs, Co_3O_4 NPs and Ag/Co_3O_4 BMNPs using *Croton macrostachyus* plant extract as a reducing agent instead of toxic chemical. Secondary metabolites in the plant extract acted as capping/stabilizing agents for the newly formed nanoparticles. The applications of both Co_3O_4 and Ag nanoparticles validate the importance of both types of nanoparticles and require further study for the well-being of humans. Though, to our knowledge no reports were published on the synthesis of Ag NPs, Co_3O_4 NPs and Ag/Co_3O_4 BMNPs by *Croton macrostachyus* plant extract through the green chemistry approach.

Therefore, in this study, the evaluation of antibacterial efficiencies and the intrinsic properties of Ag NPs, Co_3O_4 NPs and Ag/Co_3O_4 BMNPs, against certain gram positive and gram negative antibiotic-resistant bacteria were studied.

1.3. Objective

1.3.1. General objective

The main objective of this study is to synthesize, characterize and evaluate antibacterial activity of mono and bimetallic Ag NPs and Co_3O_4 NPs by using *Croton macrostachyus* plant extract.

1.3.2. Specific objective

i. To synthesize Ag NPs, Co_3O_4 NPs, Ag/Co_3O_4 BMNPs using *Croton macrostachyus* plant extract.

ii. To characterize Ag NPs, Co_3O_4 NPs, Ag/Co_3O_4 BMNPs using UV-Vis, FTIR, XRD, and SEM techniques

iii. To investigate the antibacterial activity of green synthesized Ag NPs, Co_3O_4 NPs Ag/Co_3O_4 BMNPs against Four bacterial strains: *Escherichia-coli* (gram negative), *Staphylococcus aureus* (gram positive), *Enterococcus faecalis* (gram positive), and *Salmonella typhimrium* (gram negative).

1.4. Significant of the study

Infectious diseases are one of the leading causes of death of children, adolescents and olds. The development of alarming resistance of bacteria towards antibacterial agents is a major global public health problem. Thus, we need to have effective alternate antimicrobials to fight such resistant infections. The study provides information on the role of *Croton macrostachyus* in green synthesis of Ag NPs, Co_3O_4 NPs, and Ag/Co_3O_4 BMNPs. The study could also contribute significantly to study the antibacterial activity of mono and bimetallic silver-cobalt oxide nanoparticles. The result will serve as base line for further studies related to Ag/Co_3O_4 BMNPs and their applications.

1.5. Scope of the study

This research work was limited to green synthesis of Ag NPs, Co_3O_4 NPs and Ag/Co_3O_4 BMNPs nanoparticles using *Croton macrostachyus* plant leaf extract and characterization of the nanoparticles using XRD, FTIR, SEM, TGA, and UV-Vis DRS techniques and evaluation antibacterial activity against four bacterial strains: (*Escherichia-coli* (Gram negative), *Staphylococcus aureus* (Gram positive), *Enterococcus faecalis* (Gram positive), and *Salmonella typhimurium* (Gram negative)) by Agar disc diffusion method.

2. LITERATURE REVIEW

2.1. Nanoscience and Nanotechnology

Nanoscience is the study of phenomena and manipulation of materials at atomic, molecular and macromolecular levels, where properties differs from those at a larger scale whereas Nanotechnologies are the design, characterization, fabrication and application of structures, devices and systems by controlling shape and size at nanometer level. Nano science and nanotechnologies cover such a wide range of fields (from chemistry, physics and biology, to medicine, engineering and electronics (Bowman, 2017).

According to the United States National Science Foundation; Nano science / nanotechnology studies that deals with materials and systems having the following properties: (1) Dimension: their dimension fall within the Nano-scale range of 1-100 nm. (2) Process: designed with methodologies, that displays fundamental control over the physical and chemical characteristics of molecular-scale structures. (3) Building block property: they can be form larger structure by combining together. Generally, Nano science, is quite natural in biological sciences considering that the sizes of many bio-entities we deal with (like DNA, RNA, proteins, enzymes, viruses, etc.) fall within the nanoscale range of 1-100 nm (G.Ali Mansoor, 2004).

Nanotechnology plays a significant role in many technological fields. This field has a significant contribution for manipulating the atoms or molecules and transforming them into structures having desired geometry and properties. It has both environmental and health applications which includes effective drug delivery and applications in harvesting solar energy, reducing the use of industrial chemicals and making the environment cleaner, safer and worth living. In addition to this, it can be used for water purification, cancer treatment and food packaging etc. (Sharma et al., 2019).

2.2. Nanoparticle and Nanomaterial's

Nanoparticles (NPs) and nanostructured materials (NSMs) represent an active area of research and a techno-economic sector with in many applications. NPs and NSMs have gained great technological advancements due to their tunable physicochemical characteristics like melting point, wettability, electrical and thermal conductivity, catalytic activity, light absorption and scattering resulting in enhanced performance over their bulk counterparts. Their properties

depend on their composition, size, and shape that determine their plasmonic, catalytic, and magnetic characteristics.

In principle, NMs are described as materials with length of 1–1000 nm in at least one dimension; however, they are commonly defined to be of diameter in the range of 1 to 100 nm. Now days, there are several legislations in the European Union (EU) and USA. Though, a single internationally accepted definition for NMs does not exist. Different organizations have a difference in opinion in defining NMs ((Herlekar et al., 2014; Boverhof et al., 2015).

According to US Food and Drug Administration (USFDA) states that NMs are "materials that have at least one dimension in the range of approximately 1 to 100 nm and exhibit dimension-dependent phenomena" (Guidance, D., 2011). The Environmental Protection Agency (EPA) also refers to NMs as "NMs can exhibit unique properties different than the corresponding chemical compound in a bulky dimension". The International Organization for Standardization (ISO) has termed NMs as a "material with any external nanoscale dimension or having internal nanoscale surface structure". Nanofibers, nanoplates, nanowires, quantum dots and other related terms have been defined based on this ISO definition. Likewise, the term *nanomaterial* is described as "a manufactured or natural material that possesses unbound, aggregated or agglomerated particles where external dimensions are between 1–100 nm size range", according to the EU Commission (Jeevanandam et al., 2018).

A nanoparticle can be either a zero dimensional where the length, breadth and height is fixed at a single point for example nanodots, one dimensional where it can possess only one parameter for example graphene, two dimensional where it has length and breadth for example carbon nanotubes or three dimensional where it has all the parameters such as length, breadth and height for example gold nanoparticles. The nanoparticles are of different shape, size and structure. It be spherical, cylindrical, tubular, conical, hollow core, spiral, flat, etc. or irregular and differ from 1 nm to 100 nm in size. The surface can be a uniform or irregular with surface variations. Some nanoparticles are crystalline or amorphous with single or multi crystal solids either loose or agglomerated (Anu Mary Ealia & Saravanakumar, 2017).

Nanomaterial can be classified in to: Carbon Based Materials (Sabzehmeidani et al., 2021), Metal Based Materials (Kumar et al., 2021), Dendrimers (Abbasi et al., 2014) and Composites (Janczak & Aspinwall, 2011). Carbon Based Materials are composed mostly of carbon, most commonly taking the form of a hollow spheres, ellipsoids, or tubes. Spherical and ellipsoidal

carbon nanomaterials are referred to as fullerenes, while cylindrical ones are called nanotubes. These particles have many potential applications, including improved films and coatings, stronger and lighter materials, and applications in electronics (Maiti et al., 2019). Dendrimers are nanosized polymers built from branched units. The surface of a dendrimer has numerous chain ends, which can be tailored to perform specific chemical functions. This property could also be useful for catalysis. Also, because three-dimensional dendrimers contain interior cavities into which other molecules could be placed, they may be useful for drug delivery (Abbasi et al., 2014). Composites are combined nanoparticles with other nanoparticles or with larger, bulk-type materials. Nanoparticles, such as nanosized clays, are already being added to products ranging from auto parts to packaging materials, to enhance mechanical, thermal, barrier, and flame-retardant properties (Camargo et al., 2009). Metal Based Materials include quantum dots, nanogold, nanosilver and metal oxides, such as titanium dioxide. A quantum dot is a closely packed semiconductor crystal comprised of hundreds or thousands of atoms, and whose size is on the order of a few nanometers to a few hundred nanometers. Changing the size of quantum dots changes their optical properties (Yaqoob et al., 2020).

Metal nanoparticles research has recently become the focus of intense work due to their unusual properties compared to bulk metal. Metallic nanoparticles (MNPs) have a metal core composed of inorganic metal or metal oxide that is usually covered with a shell made up of organic or inorganic material or metal oxide (Mody et al., 2010). They can be classified as monometallic, bimetallic and polymetallic nanoparticles.

2.3. Monometallic nanoparticles

Monometallic nanoparticles (MNPs), as the name suggests, consist of only single metal. The constituted metal atom determines the properties of these nanoparticles. Monometallic nanoparticles are of different types depending upon the type of metal atom present such as magnetic, metallic and transition metal nanoparticles, etc. (Sharma et al., 2019).

They can be prepared by chemical, physical and biological methods. Biological methods of NPs provide a new possibility of conveniently synthesizing NPs using natural reducing and stabilizing agents. As possible environmentally and economically friendly alternatives to chemical and physical approaches, biosynthesis of metal and semiconductor NPs using organisms has been suggested. Monodispersity and particle size and shape are very important parameters in the evaluation of NPs synthesis. Therefore, the efficient control on the

morphology and monodispersity of NPs must be explored. The reaction conditions should be optimized by using screened organisms with high production capability and controlling the reaction conditions, well- characterized NPs can be obtained by synthesis rates faster or compatible to those of chemical and physical approaches. This eco-friendly method can potentially be used in various areas, including pharmaceuticals, cosmetics, foods, and medical applications (Swain, 2016).

2.4. Bimetallic nanoparticles

In recent years, bimetallic nanoparticles are being increasingly investigated because they carry the possibility of possessing electronic, optical, magnetic and catalytic properties which may be different from the sum of the attributes of the individual particles. They can be referred to as the combination of two metals in the nanoscale size range that exhibit numerous new and improved properties (Ganaie et al., 2015). According to atomic ordering, bimetallic nanoparticles can be classified into four types:

Mixed Alloyed bimetallic Nanoparticles: They may have a random or ordered arrangement. Randomly mixed nanoalloys are often termed alloyed nanoparticles, in random structure; atoms are arranged randomly, whereas ordered mixed nanoalloys are termed intermixed or intermetallic nanoparticles (Huynh et al., 2020).

Sub-cluster segregated bimetallic Nanoparticles: These nanoparticles comprise two small clusters (sub-clusters) in their structure. There are two kinds of sub-clusters. One shares the middle interface whereas the other only shares a bone or short interface between two small clusters (Langlois et al., 2012).

Core-Shell bimetallic Nanoparticles: These nanoparticles typically consist of one metal that forms a shell surrounding a core made of another metal or the recent core–shell type which is composed of an intermixed core surrounded by a pure shell (Nelli et al., 2020). Catalysis is carried out on the nanoparticle surface. The atoms at the center are wasted. This becomes more important when expensive metals are used as catalysts. To reduce the cost of the catalysts an inexpensive metal is made the core and the catalytically active metal is taken as the shell. This is accomplished by first reducing the core metal followed by nucleation of the shell metal around it. The core metal also electronically modifies the shell and thereby improves catalytic activity. They can be synthesized by using a one-pot co-reduction method. Two metal precursors are added simultaneously. One of them will reduce first due to the

difference in the reduction potentials of the different metal ions. This metal will form the core. The pre-formed nanoparticle acts as the seed required for the nucleation of the second metal around it (Nasrabadi et al., 2014; G. Sharma et al., 2019; Blosi et al., 2016; Liu et al., 2013).

Multiple Core-Shell bimetallic Nanoparticles: These have two further kinds of multiple arrangements, multiple shell–core nanoparticles created with two or more shells covering a single core, and multiple core–shell nanoparticles with one simple shell surrounding several cores; the shell and core are always composed of two different metals. The degree of mixing and atomic ordering in bimetallic nanoparticles can be controlled by the relative strength of the bond between two chemicals, the surface energy, atomic size, electric or magnetic effects, etc. (Huynh et al., 2020).

2.5. Synthesis of nanoparticles

There are two approaches to synthesis nanomaterial of various shapes and dimensions. Namely; bottom-up and top-down approaches. In top-down methods Bulk material size is reduced to nanoparticles by different physical, chemical and mechanical processes, while bottom-up is Building up of nanomaterials from an atom by atom. The bottom-up method requires an appropriate soluble source of metals, usually metal cations in the form of soluble salts or coordinated by suitable ligands. To such a solution, a reducing agent is added whose nature has a strong influence on the particle properties (Patil et al., 2021). Moreover, they are classified into physical, chemical, and biological methods for the synthesis of NPs. The physical methods belong to the category of top-down approach, while the chemical and biological methods belong to the categories of the bottom-up approach for the synthesis NPs (Iravani et al., 2014).

2.5.1. Top-down approaches

Top-down approach is trimming down bulk material to smaller nanosized particles. Preparation of nanoparticles by this method is depend on size reduction of starting material by different physical and chemical treatments (Meyers et al., 2006). It includes methods such as mechanical milling, hydrothermal synthesis, photolithographic processing, laser ablation, and micromachining, electron beam machining, etching sputtering and electron beam lithography. Top down methods are easy to perform, is not suitable method for preparing informal shaped

and very small size particles. Change in surface chemistry and physicochemical properties of nanoparticles are major problem associated with this method (Jamkhande et al., 2019).

Mechanical milling

It is reduction of the particle size with high energy ball milling. This method of particle size reduction was developed by John Benjamin in 1970. Depending on induced mechanical energy to powder mixture, it can be classified as low energy and high energy milling that nanosized particles are generally produced using high energy ball milling process. This method is widely preferred for intermetallic nanoparticles synthesis (Jamkhande et al., 2019). In this method, bulk powder and several heavy balls added in to a container and High mechanical energy is applied on bulk powder material with the help of high speed rotating ball. Different high energy mills such as attrition ball mill, planetary ball mill, vibrating ball mill, low energy tumbling mill and high energy ball mill are used for the reduction of particles (Prasad Yadav et al., 2012).

In this method, heavy free moving high energy balls may roll down on surface of the chamber containing bulk powder material in a series of parallel layers or they may fall freely and impact the powder. It has an advantage of large scale production of high purity nanoparticles with larger physical properties such as enhanced solubility of the drug components which are poorly water soluble in a cost effective manner. It gives rise to some new and improved properties to the component relaying on their grain size and material composition (Ullah et al., 2014). However, it needs high energy and extensive long period of milling time and difficult to control the contamination of powder due to steel balls (Tavakoli et al., 2007).

Mechano-chemical synthesis

Mechano-chemical synthesis method depends on: repeated deformation, welding, and fracture of the mixture of reactants. During the milling process, different chemical modifications are produced at the interface of nanosized particles. High temperature is required to precede chemical reactions for several purposes like to separate reacting phases from the product phase. Nanoparticles can be obtained using a ball mill at low temperatures without any use of external heating (Tsuzuki & McCormick, 2004). In this method of synthesis, the starting materials are mixed stichiometrically and milled. The deformation, fraction and welding of the reactants take place during milling process. Various chemical reactions are generated at the

surface interface between substrate and reagent, and therefore the reaction that require high temperature will take place at low temperature without any external application of heat. It is a Simple and efficient method of preparation of nanoparticles (Seyedi et al., 2015). However, they may get unwanted contamination from milling media and atmosphere because the nanostructures/nanoparticles formed are highly sensitive to grinding condition and long term milling is required for the preparation of smaller particles (smaller than 20 nm) (Tavakoli et al., 2007).

Laser ablation

This method is the process of removing material from a solid (or occasionally liquid) surface by irradiating it with a laser beam. The material is heated by the absorbed laser energy and evaporates or sublimates at low laser flux while the material is typically converted to plasma at high laser flux. In this method, laser irradiation is used to reduce the particle size to nanoscale. The solid target material is placed under a thin layer and then exposed to pulsed laser irradiation (Simakin et al., 2004). The irradiation of material to laser is form fragmentation of solid material in the form of nanoparticles, which remains in liquid that surrounds the target and produces colloidal solution. This method is relatively simple and effective technique for the formation of large amount of small particles (nanosize) in the form of suspension. The relative amount of ablated atoms and particles formed are determined by laser pulse duration and energy (Kruis et al., 1998). Various parameters like time duration of laser pulse, wavelength, ablation time, laser fluency and effective surrounding liquid medium with or without surfactant influences ablation efficiency and characteristic of metal particle formed (Abou El-Nour et al., 2010).

Chemical vapor deposition

In this method thin film of gaseous reactant is deposited on the substrate at around 300-1200 °C. A chemical reaction formed between heated substrate and combining gas as an outcome thin film of product formed on the surface of the substrate. The applied pressure varies in the range of 10^2-10^5 Pascal. The advantages of this method are stiff, uniform, robust and highly pure nanoparticles are manufactured. The by-products formed on the substrate have to be conveyed back to the gaseous phase removing them from the substrate. Substrates are heated by cold wall and hot wall techniques. In the hot wall techniques, the deposition can take place

even on reactor walls. This is evaded in cold wall approach. Gas pressure and the substrate temperature affect the growth rate and quality of film (Dikusar et al., 2009).

Chemical Vapor Condensation (CVC)

Chemical vapor deposition (CVD) is a powerful technology for the synthesis of high quality solid thin films and coatings. This technique is a method where one or more volatile precursors are transported through the vapor phase to the reaction chamber, where they decompose on a heated substrate. In this method a bulk material is heated in vacuum to form a stream of vaporized and atomized matter, and either inert or reactive gas atmosphere is used. If a reactive gas such as oxygen is used, then metal oxide nanoparticles are formed. Due to their collision with the gas molecules results in the condensation and formation of nanoparticles the metal atom is rapidly cool. Gas-phase condensation uses a vacuum chamber that consists of a heating element, the metal to be made into nanopowder, powder, collection equipment, and vacuum hardware (Sun et al., 2021).

The precursor is introduced onto a heated element and is quickly melted, which is taken to temperatures far above the melting point but less to than the boiling point. Therefore an adequate vapor pressure is achieved (Chang et al., 1994). Gas is continuously introduced into the chamber and removed by the pumps, then, the gas flow moves the evaporated metal away from the hot element. As the gas cools the metal vapor, nanometer-sized particles produced. Nanoparticles form in the gas phase. The formed nanoparticles are transported by the carrier gas to the collectors (the surface of quartz rod and the wall of glass beaker) or into the liquids contained a glass beaker to form nanofluids (Wu et al., 2005). For instance Choi et al., synthesize iron nanoparticles by chemical vapor condensation (Choi et al., 2002) and Lee et al., reported synthesis of WS_2 nanoparticles by chemical vapor condensation (Lee et al., 2010)

Sputtering

This technique involves vaporizing a solid by sputtering it with an ion beam made of an inert gas. The entire process of the ion sputtering method, which forms collimated beams of nanoparticles and deposits bulk nanostructured coatings on silicon substrates, is carried out at relatively low pressures (1mTorr) (Swihart, 2003).

2.5.2. Bottom-up approaches

Sol-gel method

The sol-gel process is a more chemical method for the synthesis of many nanostructures, especially metal oxide nanoparticles. In this method, the metal precursor is dissolved in water or alcohol and converted to gel by heating and stirring by hydrolysis/alcoholysis. It should be dried using appropriate methods depending on the desired properties and application of the gel because, the gel obtained from the hydrolysis/alcoholysis process is wet or damp. This technique is capable of producing two or more types of nanoparticles in the same time, meaning that alloy products are synthesized in one step by mixing two or more metal (or metal oxide) precursors in certain proportions (Bokov et al., 2021, Adam et al., 2011). In addition, the sol-gel method makes it possible to make highly homogeneous composites with very high purity (99.99%) purity (Kajihara, 2013). When compared to conventional method, the lower temperature is process on it, so that the production of metal and ceramic nanomaterial with this method is possible in the temperature range between 70 and 320°C. The sol-gel process is a bottom-up synthesis method.

Sonochemical method

Sonochemistry uses ultrasound to develop chemical reactions. Sonochemistry formed when the ultrasound causes chemical effects on the reaction system, like the formation of free radicals that intensify the reaction (Ali Dheyab et al., 2021). High intensity ultrasound can be used for the synthesis of novel materials and provides an unusual way to known materials without high temperatures, high pressures, or long reaction times (Sáez & Mason, 2009). Compared to most approaches, this technique is very economical, allowing individual enthusiasts and researchers to experience and try out ideas. Sonochemical method is a relatively powerful and straightforward technique for producing nanomaterials, and it is possible to control the properties of nanoparticles by varying the parameters of the ultrasonic process (Jameel et al., 2020). For instance, Ali Dheyab et al. synthesized gold nanoparticle by sonochemical method (Ali Dheyab et al., 2020). Similarly, the same group discussed sonochemical synthesis of nanoparticle on iron oxide nanoparticles (Fe_3O_4 NP), gold nanoparticles (Au NP) and iron oxide-coated gold nanoparticles (Fe_3O_4@AuNP) (Ali Dheyab et al., 2021).

Co-precipitation method

Co-precipitation method is a classical the simplest approach for synthesizing iron oxide nanoparticles. This method includes simultaneous occurrence nucleation growth, coarsening and aggregation processes. Co-precipitation reactions exhibit the following characteristics: First, the products are insoluble species formed and their conditions are high super-saturation. Second, nucleation is a key step and a large amount of small particles will be formed. Third, secondary processes like Ostwald ripening and aggregation affect the size morphology and properties of the products. Forth, the super-saturation conditions essential to induce precipitation are usually the result of a chemical reaction (Kandpal et al., 2013).

The primary method of synthesis in this technique is co-precipitation, where the precursor aqueous salt solution is mixed with a base under an inert atmosphere at room temperature or elevated temperature. The formed nanoparticle is dependent on the type of bases used. As compared with other synthesis routes, co-precipitation is more facile and suitable. After the formation of MNP, the surfactant is added immediately to protect the synthesized MNP from being oxidized. They can be used as a stabilizing agent by preventing them from agglomeration (Petcharoen & Sirivat, 2012). Mohammadi et al., synthesize magnetite nanoparticles by co-precipitation method (Mohammadi et al., 2021), Mohanapriya et al. also reported ZnS nanoparticles by co-precipitation method (Mohanapriya et al., 2020) as for instance.

2.6. Biological Synthesis of NPs

Biological Synthesis of NPs is the use of methods and techniques to decrease the generation or use of feedstock, byproduct, product, reagents, and solvents, etc. that are dangerous to human health or to the environment (Ismail et al., 2018). The biosynthetic route is a safe, biocompatible, environment-friendly green approach to synthesize nanoparticles using plants and microorganisms for biomedical applications (Ahmed et al., 2016). This synthesis can be carried out with as plants and plant products, algae, fungi, yeast, bacteria, and viruses (Narayanan & Sakthivel, 2011). The major limitations of physical methods are expensive operations low production rate, and high energy consumption. The chemical methods are economical for large-scale production; but, the use of toxic chemicals and production of harmful by-products cause environmental damage, thereby limiting its clinical and biomedical applications (Banne et al., 2017).

2.6.1. Plant-mediated synthesis of NPs

For the synthesis of nanoparticles, it is necessary to replace toxic chemicals by biomolecules or through biogenic processes which is an efficient strategy to overcome the aforementioned limitations. Among different living organism, plants are the best choice for the synthesis of NPs due to their simplicity and easy handling (Kuppusamy et al., 2016). Phytochemicals (polyphenols, terpenoids, flavones, amino acids, alkaloids, aldehydes, flavones, ketones, proteins, phenolics, polysaccharides, saponins, tannins, terpenoids, and vitamins) in the plants are responsible for the synthesis of metal nanoparticles. The reducing capping/stabilization properties of plant phytochemical make the metal nanoparticles eco-friendly; cost effective and biocompatible. Synthesis of nanoparticles by plant mediated can be achieved by three different ways: (i) intracellularly- inside the plant, (ii) extracellularly-using plant extracts, and using individual phytochemicals. Several plants have the ability of metal accumulation and successive conversion of these accumulated metals to NPs intracellularly (Patra et al., 2017, Akinsiku et al., 2020, Dikshit et al., 2021).

The plant extracts are prepared by different methods like hot extraction, cold extraction, and using Soxhlet apparatus, which were later used in NPs synthesis. The synthesis of metal NPs is prepared by adding the plant extract to the metal precursor solution containing the salts of individual metals. The synthesis of metal NPs using plant extract mostly occurs in three stages. In the first, the reduction of metal ions (M^{+} or M^{2+}) to metal atoms (M^{0}) and successive nucleation of the reduced metal atoms occurs. The reduction of metal ions (M^{+} or M^{2+}) to metal atoms (M^{0}) and subsequent nucleation of the reduced metal atoms occurs in the first step, and the combining of tiny nearby NPs into larger size particles occurs in the second step. Finally, the termination of the process takes place while giving the final shape to the NPs (Makarov et al., 2014, Si & Mandal, 2007).

2.6.2. Microorganism mediated synthesis of NPs

Microorganisms have the ability to accumulate and detoxify heavy metals because several reductase enzymes are present which are able to reduce metal salts to metal nanoparticles. When compared to physicochemical methods, this method is environmentally friendly, inexpensive, clean and non-toxic tools that do not require much energy for synthesis of nanoparticles (Singh et al., 2016).

Not all microorganisms are able to produce nanoparticles because they are produced through metabolic pathways and through cellular enzymes that may not be present in some organisms. The synthesis of nanoparticles also depends on the capacity of microorganisms for tolerating heavy metals. High metal stresses can affect several microbial activities and some microorganisms have the capability to reduce metal ions to the appropriate metals under stress condition. Because of their absorption and chelation by intracellular and extracellular proteins, bacteria that live in metal-rich ecosystems are typically extremely resistant to those metals. Consequently, this method, which mimics the natural bio-mineralization process, could be a favorable approach for the nanoparticles synthesis. The presence of diverse components such as enzymes, proteins, and other biological molecules in microorganisms also play an important role in the process of reducing nanoparticles (Mohd Yusof et al., 2019).

Intracellular biosynthesis involves unique transport systems in microorganisms in which the cell wall plays an important role due to its negative charge: positively charged metal ions are deposited in negatively charged cell walls through electrostatic interactions. After transport into the cells of the microorganism, ions are reduced using metabolic reactions mediated by enzymes such as nitrate reductase to forms Nanoparticles. The nanoparticles accumulated in the periplasmic space can then be passed through the cell wall. The extracellular biosynthesis of Nanoparticles is also a nitrate reductase-mediated synthesis in which the nanoparticles are produced by reductase enzymes which are either located in the cell wall or secreted from the cell to the growth medium. In this process the nitrate reductase reduces metal ions to the metallic forms (Hulkoti & Taranath, 2014).

Studies have shown that NADH-dependent enzymes are responsible for the nanoparticles synthesis. The reduction mechanisms seem to begin by transferring an electron from NADH by NADH-dependent reductases as the electron carrier (Jain et al., 2011). In addition, proteins secreted by microorganisms can act primarily as a stabilizing agent and provides colloidal stability while preventing agglomeration of Nanoparticles (Mohd Yusof et al., 2019). The main drawbacks of microorganism-based synthesis of nanoparticle are complicated steps such as microbial sampling, isolation, culturing and storage. Additionally, the recovery of nanoparticles produced by this method requires downstream processing (Singh et al., 2016).

Green Synthesis of silver nanoparticles

Silver is one of the most commercialized nanomaterial with five hundred tons of silver nanoparticles production per year (Larue et al., 2014) and is estimated to increase in next few years. Its profound role in field of high sensitivity bimolecular detection, catalysis, biosensors and medicine; it has been acknowledged to have strong inhibitory and bactericidal effects along with the anti-fungal, anti-inflammatory and anti-angiogenesis activities (Veerasamy et al., 2011).

Plant extract of *Vernonia amygdalina Del.* (Desalegn et al., 2020), *Tropaeolum majus* (Bawazeer et al., 2021,) marigold flower (Padalia et al., 2015), Z*ziziphora tenuior* (Sadeghi & Gholamhoseinpoor, 2015), *Erythrina indica* (Rathi Sre et al., 2015), beet root (Bindhu & Umadevi, 2015), *Ocimum tenuiflorum* (Logeswari et al., 2015), *Spirogyra varians* (Salari et al., 2016), are some reported literatures for the synthesis silver nanoparticles.

The primary requirement of green synthesis of Ag NPs is silver metal ion solution and a reducing biological agent. In most of the cases reducing agents or other constituents present in the cells acts as stabilizing and capping agents, so there is no need of adding capping and stabilizing agents from outside. The Ag^+ ions are primary requirement for the synthesis of Ag NPs which can be obtained from various water soluble salts of silver.

Green synthesis of Co_3O_4 nanoparticles

Cobalt and cobalt oxide (Co_3O_4) NPs have been exploited extensively because of their unique and wide range of applications (Iravani et al., 2014). Co_3O_4 is an antiferromagnetic p-type semiconductor with multifunctional applications such as biomedical applications (antibacterial, anti-viral, antifungal, antileishmanial, therapeutic agents, anti-cancer, and drug delivery), gas sensors, solar selective absorbers, anode materials in lithium-ion batteries, energy storage, pigments and dyes, field emission materials, capacitors, heterogeneous catalysis, magneto-resistive devices, and electronic thin films (Kumar et al., 2014; Li et al., 2010; Waris et al., 2021).

Ahmadov et al. reported the synthesis of Co_3O_4 nanocrystals from freshly extracted ovalbumin with 8–17 nm (Ahmadov et al., 2011). Sun et al. also reported the synthesis of Co_3O_4 NPs using egg-albumin (J. Sun et al., 2019). Hosein et al. reported the synthesis of Co_3O_4 NPs with a uniform shape and size using ferritin (Hosein et al., 2004).

Green synthesis of silver-cobalt bimetallic nanoparticles

Bimetallic silver-cobalt (Ag-Co) has gained interest in different branches of science and industry, including catalysis (Aazam & Zaheer, 2022; Ai et al., 2015), biotechnologies, and energy storage and conversion devices such as fuel cells, batteries, etc. Different techniques have been used for the preparation of bimetallic Ag-Co, including, chemical reduction (Parang & Moghadamnia, 2019), hydrothermal reduction, sol-gel, inter-matrix synthesis (Ashok et al., 2018), co-precipitation (Iqbal et al., 2021). Erdogan et al. synthesized bimetallic Ag-Co using a co-precipitation method and studied the catalytic oxidation of carbon monoxide (Gulari et al., 1999). Akinsiku et al. synthesized Ag/Co bimetallic nanoparticles using aqueous leaf extract of *Canna indica* at room temperature (Akinsiku et al., 2018). Danbature et al. reported the green synthesis of silver-cobalt bimetallic nanoparticles by root extract of palmyra palm. The synthesized NPs showed potential control for larval population growth (Danbature et al., 2020). Ag-Co bimetallic nanoparticles prepared by simultaneous reduction of $Co(NO_3)_2$ and $AgNO_3$, using sodium borohydride ($NaBH_4$) as reducing agent. The developed electro-catalyst was found to be active for the direct electrochemical reduction of gaseous CO_2 (S. Singh et al., 2017).

2.7. Anti-bacterial action of nanoparticles

Metal NPs have the ability to discern bacterial from mammalian cells because of the cells' capacity to diverge metal transport systems and metallo-proteins. Metal-based NPs can personalize bacterial efficiency by various mechanisms. Those are; cell membrane degradation through electrostatic interactions, disturbance in homeostasis through protein binding, reactive oxygen species (ROS) generation and oxidative stress, disruption of proteins and enzymes, genotoxicity, and signal transduction inhibition. Retardation of bacterial growth is accomplished either by one or by combination of the above mechanisms depending on the nature and chemistry of the metal NPs involved (Baptista et al., 2018; Chen et al., 2014). Consequently, multi action effects are possible by combining more than one metal type in the same nanostructured system.

Anti-bacterial action of silver nanoparticles

Nanoscale silver particles with high surface-area-to-volume ratio (size below 100 nm) are of prime interest due to high antimicrobial actions against both Gram-positive and Gram-negative bacteria, viruses and other eukaryotic microorganisms as compared to other metals in

their nano size. It also offers potential effects against multidrug susceptible as well as multidrug resistant strains like *Pseudomonas aeruginosa*, *ampicillin-resistant Escherichia coli*, *erythromycin-resistant Streptococcus pyogenes*, *methicillin-resistant Staphylococcus aureus* (MRSA) and *vancomycin-resistant Staphylococcus aureus* (VRSA (Roy et al., 2019). Microbes are unlikely to develop resistance against silver, because the metal attacks a broad range of target sites in the organisms. Ag NPs target both the respiratory chain and the cell-division machinery, while concomitantly releasing silver ions (Ag^{+}) that increase bactericidal activity and finally leading to cell death (Padilla-Cruz et al., 2021).

Kambale et al. reported that silver nanoparticles (Ag NPs) were synthesized using aqueous leaf extracts of three Congolese plant species, namely *Brillantaisia patula* (BR-PA), *Crossopteryx febrifuga* (CR-FE) and *Senna siamea* (SE-SI). The Ag NPs derived from BR-PA, CR-FE and SE-SI exhibited higher antibacterial activity against three bacterial pathogens of the human skin compared to their respective crude extracts and $AgNO_3$ (Kambale et al., 2020).

Mehwish et al. reported the green synthesis of silver nanoparticles (Ag NPs) using Moringa oleifera seed (MOS) as a reducing/capping agent. The MOS-Ag NPs showed excellent antimicrobial activity against Gram positive (*Staphylococcus aureus* 14.6 mm) and Gram negative (*Escherichia coli* 30.6 mm, *Salmonella enterica typhimurium* 29 mm), and *Pseudomonas aeruginosa*; 22.8 mm) bacteria. Moreover, the MOS-Ag NPs showed remarkable photo catalytic activity toward organic dyes (methylene blue (> 81%), orange red (> 82%), and 4-nitrophenol (> 75%)) under sunlight irradiation. In addition, > 80% of the toxic lead metal ions was removed from the treated water by MOS-Ag NPs. Under similar conditions, the synthesized MOS-Ag NPs retained their photo catalytic efficiency after 10 photo catalytic cycles. Overall, these findings indicate that MOS-Ag NPs may be a powerful antimicrobial agent against water borne pathogens as well as a promising and economic agent for use in the treatment of waste generated by industrial dyeing processes (Mehwish et al., 2021).

Anti-bacterial action cobalt nanoparticles

Eltarahony et al. reported the green synthesis of combined Co NPs using gram-negative bacteria *P. mirabilis*. The characterization of NPs was confirmed by UV-Vis, EDX, XRD, TEM, dynamic light scattering (DLS), and polydispersity index (PDI). The antibacterial

activity was observed using a well diffusion assay against *S. typhiea, E. coli, C. perfringens, S. aureus,* and *Enterococcus faecalis*. The result showed that the NPs have promising biocide efficiency against these bacteria (Eltarahony et al., 2018).

Omran et al. synthesized quasi-spherical shape cobalt oxide NPs with an average size of 20-27 nm diameter using a fungal specie *Aspergillus brasiliensis.* The first-time m*ycosynthesized* cobalt oxide NPs showed considerable activity against different bacteria (Omran et al., 2019).

Biogenic synthesis of Co NPs using *Celosia argentea* whole plant extract has been reported and studied for their antibacterial activities using the disk diffusion method. The synthesized NPs

showed remarkable antibacterial activities against *B. subtilis* and *E. coli* (Shahzadi et al., 2019)

Green-mediated cobalt oxide NPs have been synthesized using *Hibiscus rosa-sinensis* flower extract and their antibacterial activity was measured. These green synthesized NPs showed promising activities against *E. coli, Streptococcus mutans, S. aureus*, and *Klebsiella pneumonia* (Anuradha & Raji, 2019).

Anti-bacterial action of silver-cobalt bimetallic nanoparticles

Boroujeni et al. reported the synthesized Ag/Co nanoparticles by chemical reduction method show good antibacterial properties (Boroujeni et al., 2019). Janani et al. also revealed the synthesized Ag/Co- polyvinyl pyrrolidone Nano composites showed excellent antibacterial activity against both Gram negative (*B. subtilis*) and Gram positive (*E. coli*) bacteria (Janani et al., 2020).

2.8. Plant description and ethno botanical use

Croton *macrostachyus* (Broad-leaved Croton) is a species of the genus Croton *L.*, *Euphorbiaceae* family, called Croton under the sub family *Crotonoideae*, which comprises more than 1200 species of herbs, shrubs, trees, and occasionally lianas. It is widely distributed in tropical Africa, from Guinea east to Ethiopia and Somalia, south to Angola, Mozambique, and Madagascar. The species has been reported to occur in Angola, Burundi, Cameroon, Central African Republic, Democratic Republic of Congo (DRC), Ethiopia, Rwanda, Tanzania Ghana, Guinea, Sudan Ivory Coast, Kenya, Madagascar, Malawi, Mozambique, Nigeria, Somalia, South Sudan, Uganda, and Zambia. *C. macrostachyus* plant is common in secondary

forests, particularly on forest edges and along rivers or lakes, in moist or dry evergreen upland forest, woodland, wooded grassland, bushland, and along roadsides, often on soils of volcanic origin at altitude between 200 to 3400 m above sea level and mean annual rainfall between 150 mm and 1200 mm (Maroyi, 2017).

In Ethiopia, *Croton macrostachyus* occurs in regions between 1300 and 2500 m above the sea level, with an annual rainfall ranging between 750 and 2000 mm. The tree is common in the secondary forests, forest edges, riversides, lakesides, wet regions, dry evergreen upland forests, woodlands, grasslands, bushlands and as well, along the roadsides (Wakjira & Negash, 2013). *Croton macrostachyus* prevents the soil erosion and serves as a traditional medicine to cure abdominal ache, scabies, bleeding, constipation, dermatophilosis, epilepsy, rabies, warts, and wounds (Aga et al., 2020). The ethno medical use of *Croton macrostachyus* leaves include antimicrobial, antioxidant activity the flowers are shows antimicrobial activity, antioxidant activity (Obey et al., 2016). However, no research has been reported on the biosynthesis of nanoparticles mediated by *Croton macrostachyus* plant.

Figure 1: *Croton macrostachyus* plant

Phytochemical information on the *Croton macrostachyus*

Previous chemical analyses of the plant indicate the presence of alkaloids, amino acids, anthraquinones, carbohydrates, cardiac glycosides, coumarins, essential oil, fatty acids, flavonoids, phenolic compounds, phlobatannins, polyphenols, phytosteroides, saponins, sterols, tannins, terpenoids, unsaturated sterol and vitamin C have been identified from *C. macrostachyus* fruits, leaves, stem bark, and twigs (Degu et al., 2016; Obey et al., 2016).

3. MATERIALS AND METHOD

In this chapter, materials, chemicals and methods of the experiments were presented. The first part of the chapter covered various chemicals, samples and instruments required to carry out this research and in the second section of this chapter, synthesis methods of different samples for Ag NPs, Co_3O_4 NPs and Ag/Co_3O_4 BMNPs synthesis and finally the method to test antibacterial activity of the prepared nanoparticles were presented.

3.1. Materials

The following were among the various chemicals, samples, and laboratory apparatus used for this Thesis work.

3.1.1. Chemicals

The chemicals and reagents required for the preparation of Ag NPs, Co_3O_4 NPs and Ag/Co_3O_4 BMNPs were distilled water, cobalt(II) nitrate hexahydrate ($Co(NO_3)_2.6H_2O$, silver nitrate ($AgNO_3$), ethanol, sodium hydroxide (NaOH), Muller Hinton agar, Sulfuric acid (H_2SO_4), Ferric Chlorid ($FeCl_3$) and *Croton macrostachyus* plant extract. All the chemicals were analytical grade. The chemicals and reagents were bought from chemical stores in Addis Ababa and *Croton macrostachyus* plant was collected from its natural habitat areas of Oromia Regional State, West Showa, Adea Berga Woreda.

3.1.2. Apparatus and Instrumentations

3.1.2.1. Apparatus

The following laboratory apparatus were used for the experiments: beaker, measuring cylinder, pipettes, pH meter, volumetric flasks, magnetic stirrer with hot plate, funnel, filter paper, analytical balance, dropper, centrifuge, Test tube, spatula, conical flask, Petri-dish, micropipette and crucible.

3.1.2.2. Instruments

The laboratory instruments that were used for characterizing the synthesized NPs were: UV-Vis spectroscopy which was used to study the optical properties of the nanoparticles, FITR was used to characterize the vibrational motions of atoms in the molecules of the synthesized Ag NPs, Co_3O_4 NPs and Ag/Co_3O_4 BMNPs, XRD was used to characterize the nature of

crystal structure of the synthesized nanoparticles, SEM was used to show the morphology of the synthesized nanoparticles and TGA/DTA was used to analysis thermal stability of the synthesized nanoparticles.

3.2. Methods

3.2.1. Preparation of the *Croton macrostachyus* Plant Extract

The *Croton macrostachyus* plant leaf was collected from its natural habitat areas of Oromia Regional State, West Showa, Adea Berga Woreda. Sample collection and preparation of *Croton macrostachyus* leaves extract were carried out according to the literature of (Riaz et al., 2020) with slight modifications. *Croton macrostachyus* leaves were collected and the fresh leaves were washed thoroughly with deionized water to remove any dirt particles. The washed leaves were air-dried and grounded. 18 g of *Croton macrostachyus* plant leaves powder was added into 1000 mL conical flask and then 600 mL of distilled water was also added to the flask; then the mixtures were heated to 70 ^{o}C for 30 min. After 30 min, the heater was turned off and the mixtures were stirred for 1 hr. After a while, the mixture was allowed to settle. Then after settlement, the extract was filtered with whatman no.1 filter paper and kept in refrigerator at 4 ^{o}C. Then, the prepared extract was used for the synthesis of Ag NPs, Co_3O_4 NPs and Ag/Co_3O_4 BMNPs. Figure 2 shows schematic procedure for the preparation of the plant extract.

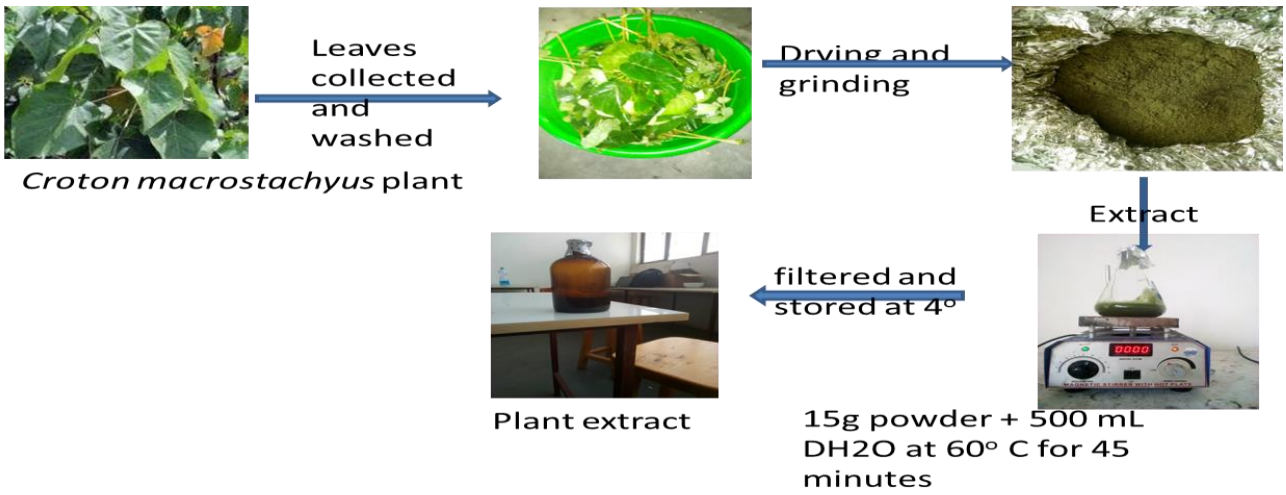

Figure 2: Preparation of *Croton macrostachyus* plant extract

3.2.2. Phytochemical Qualitative Analysis of Aqueous Extract *Croton macrostachyus* plant

The plant extract was subjected to assessment for the existence of the phytochemicals by using the following reported standard methods (Yadav et al., 2011; Adetunji et al., 2013)

Tests for Flavonoids (Alkaline Reagent Test): 2 mL of 2.0% NaOH mixture was mixed with aqueous plant crude extract; concentrated yellow color was produced, which became colorless when 2 drops of diluted acid were added to the mixture. This result showed the presence of flavonoids.

Test for tannins (Ferric chloride test): 2 mL Plant extract was taken in test tube and boiled. 5 drops of 0.1% $FeCl_3$ were added to give a brownish-green or a blue-black color which confirms the presence of tannins.

Test for terpenoids (Salkowski test): 2 mL of aqueous plant extract was mixed with 2 mL of chloroform and 3 mL concentrated H_2SO_4 carefully to form a layer. A reddish-brown coloration of the interface was formed to show positive results for the presence of terpenoids.

Test for Steroids: 2 mL of chloroform and concentrated H_2SO_4 were added with the 5 mL aqueous plant crude extract. In the lower chloroform layer, the red color appeared that indicated the presence of steroids.

Tests for Glycosides (Salkowski's Test): 2 mL concentrated H_2SO_4 was added to aqueous plant extract. A reddish-brown color formed which indicated the presence of steroidal aglycone part of the glycosides.

Test for phytosterols (Salkowski's test): 2 mL of aqueous plant extract and 10 mL of chloroform were added and then filtered. 5 drops of concentrated H_2SO_4 were added to the filtrate; the mixture was shaken and examined for the appearance of the golden yellow color.

Test for saponins: 0.5 g of plant extract was taken then 5 mL of distilled water was added and shaken while heating to boil. Frothing showed the presence of saponins.

Test for phenols: 5 drops of 2% of $FeCl_3$ were added to 2 mL of aqueous plant extract and the formation of bluish-green to black color indicates the presence of phenols.

3.2.3. Procedure for synthesis of silver Nanoparticles

Synthesis of silver nanoparticles using *Croton macrostachyus* leaf extract were carried out using to the reported procedure (Murthy et al., 2020) with minor modification. For the synthesis of silver nanoparticles, aqueous solution (0.2 M) of $AgNO_3$(aq) solution was prepared by taking 16.987 g of $AgNO_3$ salt and added into 500 mL of volumetric flask then distilled water was added and shaken to get a homogenous mixture. Finally, the distilled water was filled into the volumetric flask until its mark and used for the synthesis of silver nanoparticles**.** The Ag NPs were prepared by mixing 200 mL of 0.2 M silver nitrate solution with 200 mL of *Croton macrostachyus* plant extract under stirring at 30 °C for 3 hr. The mixture was settled at room temperature for 24 hr and then, the solution was centrifuged for 20 min at 2000 rpm. Then, the solid part was washed with distilled water and ethanol then dried on a ceramic crucible for 24 hr at 70 °C in oven. Finally, the powder of dark brown color was obtained and stored for further analysis.

Figure 3: Synthesis of silver nanoparticle

3.2.4. Procedure for synthesis of Co_3O_4 Nanoparticles

Synthesis of Co_3O_4 nanoparticles using *Croton macrostachyus* leaf extract were carried out according to the literature report by (Samuel et al., 2020) with minor modification. For the synthesis of Co_3O_4 NPs, aqueous solution (0.2 M) of $Co(NO_3)_2.6H_2O$(aq) solution was prepared by taking 29.1 g of $Co(NO_3)_2.6H_2O$) salt and added into 500 mL of volumetric flask then distilled water was added and shaken to get a homogenous mixture. Finally, the distilled water was filled into the volumetric flask until its mark and used for the synthesis of Co_3O_4 NPs**.** The Co_3O_4 NPs were prepared by mixing 200 mL of 0.2 M $Co(NO_3)_2.6H_2O$ solution with 200 mL of *Croton macrostachyus* leaf extract under stirring at 60 °C for 5 hr. The pH was monitored using the pH meter, and 30 mL of 1 N of NaOH was added as a precipitating agent followed by stirring for about 20 min. The mixture was settled at room temperature for 24 hr and then, the solution was centrifuged for 20 min at 2000 rpm. Then, the solid part was washed with distilled water and ethanol then dried on a ceramic crucible for 24 hr at 70 °C in oven. Finally, the powder of light-brown color was obtained then, the powder was calcinated at 400 °C for 4 hr and the obtained result was used for further analysis.

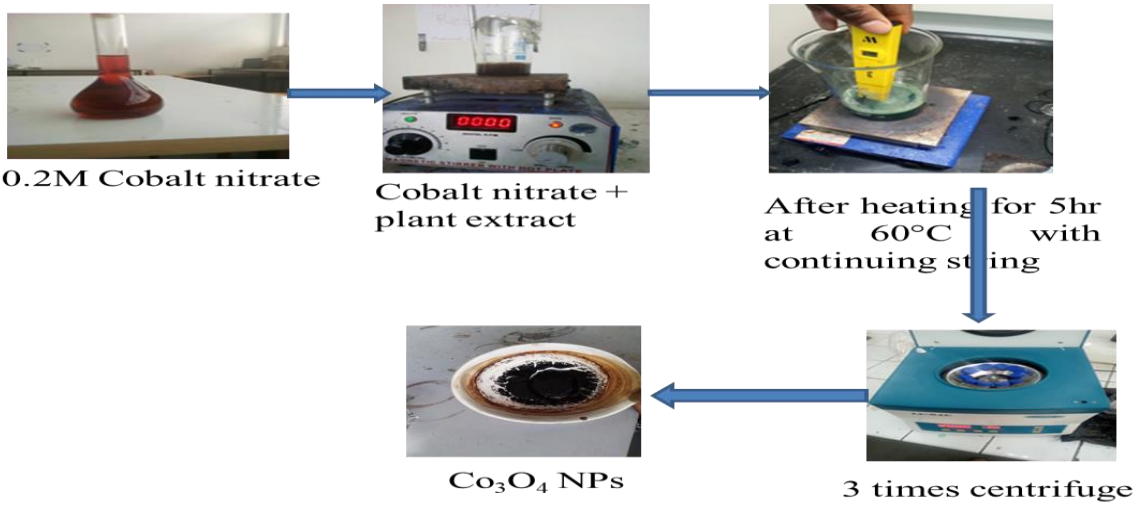

Figure 4: syntheses of Co_3O_4 NPs

3.2.5. Procedure for synthesis of bimetallic nanoparticles

Synthesis of Ag/Co_3O_4 BMNPs using *Croton macrostachyus* leaf extract were carried out according to the literature of (Danbature, Shehu, & Adam, 2020) with minor modification. For the synthesis of Ag/Co_3O_4 BMNPs, 100 mL of 0.2 M $AgNO_3$ solution was added to the 1000

mL beaker. Then, 100 mL of 0.2M $Co(NO_3)_2.6H_2O$ solution was added to the beaker while stirring for 15 min. After 15 min 200 mL of plant extract was added to the solution slowly while heating at 60 °C for 5 hr. The pH was monitored using the pH meter, and 30 mL of 1 N of NaOH was added as a precipitating agent followed by stirring for about 20 min. Then the mixture was settled at room temperature for 24 hr and the solution was centrifuged for 20 min at 2000 rpm. Then, the solid part was washed with distilled water and ethanol then dried on a ceramic crucible for 24 hr at 70 °C in oven. Finally, the powder of black-brown color was obtained then, the powder was calcinated at 400 °C for 4 hr and the obtained result was used for further analysis.

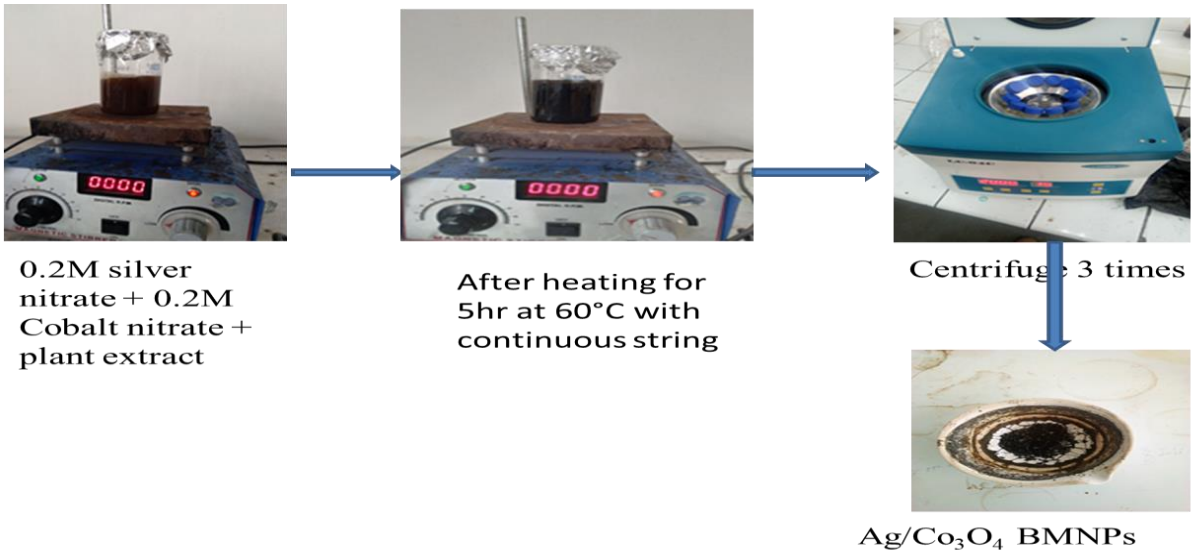

Figure 5: Syntheses of Ag/Co_3O_4 BMNPs

3.2.6. Procedure for Antibacterial activity test

The synthesized Ag NPs, Co_3O_4 NPs and A55g/Co_3O_4 BMNPs were screened for *in vitro* antibacterial activities against four bacteria strains (*Escherichia-coli (*Gram negative), *Staphylococcus aureus* (Gram positive), *Enterococcus faecalis* (Gram positive), and *Salmonella typhimurium* (Gram negative)) by Agar disc diffusion method (Linh et al., 2018) at Adama public health referrals and research laboratory center. The bacterial stock cultures were maintained on the sheep blood agar slants at 37 ^oC. Freshly, grown liquid culture of the test strains having similar turbidity with 0.5 McFarland were seeded over the Mueller-

Hinton agar medium with sterile swab. The disc measuring 6 mm in diameter was prepared from Whatmann filter paper sterilized by dry heat at 121 ^{o}C for 20 min. The different concentrations of Ag NPs, Co_3O_4 NPs and Ag/ Co_3O_4 BMNPs (20, 10, 5 and, 2.5 mg/mL) were prepared by dissolving synthesized nanoparticles in DMSO. Then, sterilized 6 mm filter paper discs were soaked in each prepared nanoparticles. The discs impregnated with the test solutions were placed on a cultured glass plate at equal distance to one another to avoid overlap of zones of growth inhibitions.

The growth inhibition zone was measured in mm after 24 hr incubation at 37 ^{o}C and compared with the standard drug Contrimoxazole. DMSO was used as a negative control and 25 µg Contrimoxazole was used as a standard drug. All the above procedures were repeated three times and mean standard deviation of a zone of inhibition were taken.

4. RESULTS AND DISCUSSION

In the first section of this chapter, the results of the phytochemical screening of *Croton macrostachyus* plant extract were presented. In the second section, crystal size, lattice parameters, micro-strains and dislocation densities of Ag NPs, Co_3O_4 NPs and Ag/Co_3O_4 BMNPs by X-ray diffraction were presented. In the third section, the UV-Vis absorption spectra and calculated band gaps of those synthesized NPs were presented. In the fourth section of this chapter, the SEM analysis was discussed. In the fifth section, the functional groups and their assignments of synthesized NPs were presented briefly. In the sixth section the thermal stability of the synthesized nanoparticles were presented. In the last section, the antibacterial activities of the synthesized nanoparticles were discussed.

4.1. The Phytochemical screening test results

The preparation of the *Croton macrostachyus* plant extract by aqueous extraction of the dried and ground plant was the initial activity carried out for the green synthesis of the metallic and bimetallic nanoparticle. Then to understand the phytochemicals responsible for the reduction and/or capping during the synthesis of the nanoparticles, the phytochemical screening of the extracted *Croton macrostachyus* plant extract has been carried out. Accordingly, the results of the phytochemical analysis for the extract of *Croton macrostachyus* plant are summarized in Table 1 supported by figure 6.

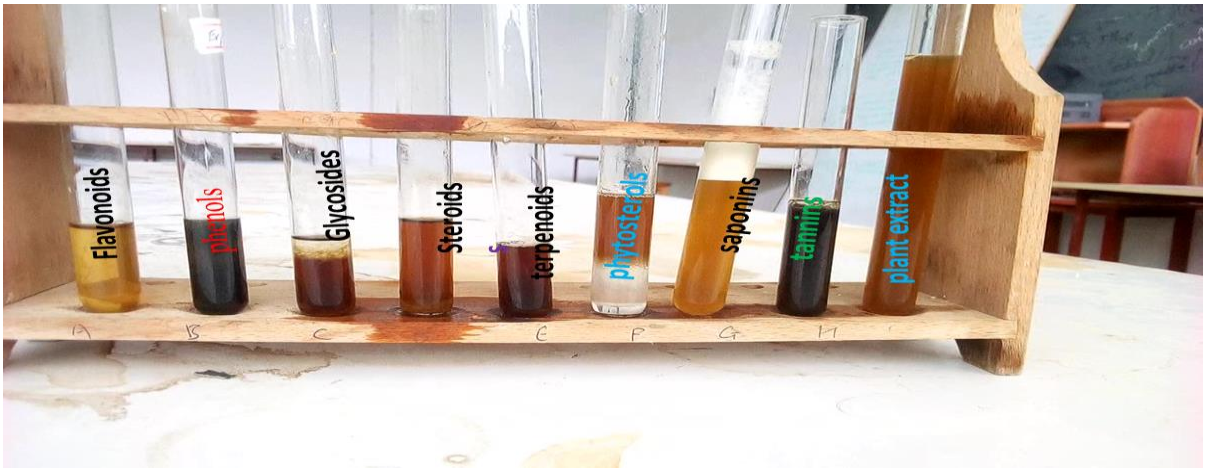

Figure 6: Results of phytochemical screening of *Croton macrostachyus* plant extract

Table 1: Results of phytochemical screening of *Croton macrostachyus* plant extract

s.no	Secondary Metabolite	Results
1	Flavonoid	+
2	Tannins	+
3	Terpenoid	+
4	Steroid	+
5	Phytosterols	+
6	Glycosides	+
7	Sapponins	+
8	Phenols	+

The data obtained revealed that the *Croton macrostachyus* plant extract was primarily composed of flavonoids, tannins, terpenoids, glycosides, phytosterols, saponins and phenols which are responsible for the facilitation of the synthesis of Ag NPs, Co_3O_4 NPs and Ag/Co_3O_4 BMNPs. The Phyto-components of plant extracts act as reducing as well as stabilizing agents (Ovais et al., 2018).

The flavonoids can be used as reducing agents for the preparation of biocompatible NPs (Zhou et al., 2010). Ahmad et al., (2010) revealed that free hydrogen produced during the ketoenol conversion of flavonoids, i.e., luteolin and rosmarinic acid, can be reduce Ag^+ ions for producing silver NPs (Ahmad et al., 2010). A similar report showed that the –OH group of flavonoids (quercetin and myricetin) during the bioreduction of metal ions can be oxidized to carbonyl groups (Ghoreishi et al., 2011). Polyphenols and terpenoid are used as both bioreducing and stabilizing agents. Plant extracts rich with saponins, tannins, glycosides, phytosterol can support synthesis of small size nanoparticles (Raja et al., 2017; Mashwani et al., 2016).

4.2. X-ray diffraction (XRD) analysis

X-ray diffraction (XRD) analysis was performed to determine the composition and crystal structure of the synthesized Ag NPs, Co_3O_4 NPs and Ag/ Co_3O_4 BMNPs. Figure 7 shows the XRD results of the prepared samples. The patterns obtained experimentally were identified through comparison with the standard Ag NPs, Co_3O_4 NPs patterns. For Ag NPs diffraction

peaks were observed at 2θ values, 38.15°, 44.23°, 64.48° and 77.39° which corresponds to (111), (200), (220) and (311) plane respectively as shown figure 7(a). The spectral data revealed that the synthesized Ag NPs showed cubic phase and the observed peaks were fitted with the Joint Committee on Powder Diffraction Standard (JCPDS card No. 004-0783), space group Fm-3m).

The XRD pattern of Co_3O_4 NPs is presented in figure 7(b) and in the difractogram, the diffraction peaks were observed at 2θ =19.19°, 31.47, 37.07°, 38.73°, 44.96°, 55.73°,59.47°, 65.34° and 77.42° corresponding to the miller indices (hkl) values of (111), (220),(311), (222), (400), (422), (511), (440), and (533) respectively. The spectral data obtained showed that the synthesized Co_3O_4 NPs showed cubic spinel crystal structure phase and the observed peaks were fitted with the Joint Committee on Powder Diffraction Standard (JCPDS card No. 042-1467, space group Fd-3m).

The XRD diffraction pattern of Ag/Co_3O_4 BMNPs is presented in figure 7(c). The peaks at 2θ values 19.15°, 31.33°, 36.91°, 38.18°, 44.37°, 59.36°, 64.53°, and 77.44° corresponding to the miller indices (hkl) values of (111), (220), (311), (111), (200), (511), (220) and (311) respectively. The diffraction peaks at 2θ values of 38.18°,44.38°, 64.53° and 77.44° are associated with the (111), (200), (220) and (311) planes of face-centered cubic (FCC) Ag (JCPDS card No. 004-0783), and the peaks at 19.15°, 31.33°, 36.91° and 59.36° correspond to the miller indices of (111), (220), (311) and (511) are planes of Co_3O_4 (JCPDS card No. 042-1467) confirming that the synthesized Ag/Co_3O_4 BMNPs nanostructures have a crystalline structure. It can be seen that both Ag and Co_3O_4 peaks can be found in the sample. The relatively intensities of the Co_3O_4 peaks decreased compared to those of the Ag peaks is due to formation of the Ag shell coating on the Co_3O_4 core surface (Jin et al., 2016).

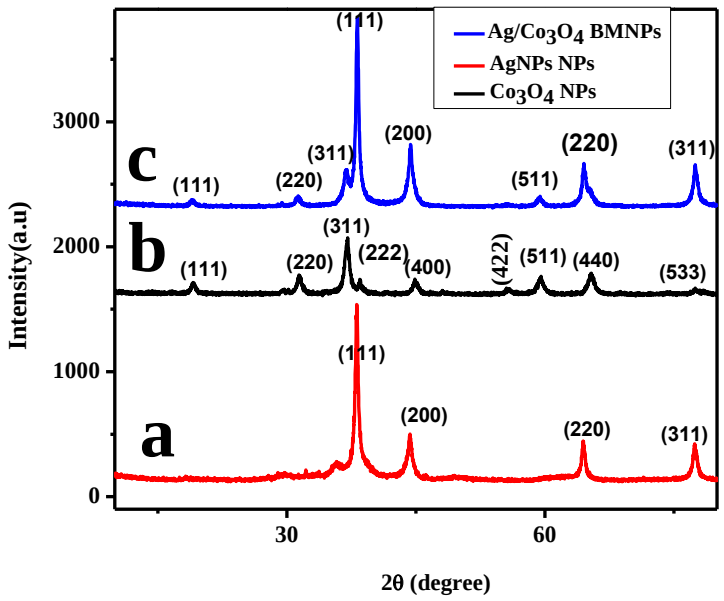

Figure 7: X-ray diffraction patterns a) Ag NPs, b) Co_3O_4 NPs and c) Ag/Co_3O_4 BMNPs.

The average crystallite size of the prepared nanoparticles is estimated by using Scherrer"s formula (Vorokh, 2018) equation (1).

$$D = \frac{K\,\lambda}{\beta\,\cos\theta} \qquad (1)$$

Where D is average crystallite size $K = \frac{2\sqrt{(ln2)}}{\pi}$ is average particle size, θ is the Bragg diffraction angle, λ is the X-ray wavelength (CuKα radiation and equals to 0.15406 nm), β is the FWHM of the XRD peak appearing at the diffraction angle θ.

The dislocation densities of synthesized NPs are calculated from;

$$\delta = \frac{1}{D^2} \qquad (2)$$

Where δ is the dislocation density, D is the crystalline size.

For the synthesized Ag NPs, Co_3O_4 NPs and Ag/Co_3O_4 BMNPs the d-spacing (d), particle size (D) and dislocation density (δ) were calculated and presented in the table (2-4) below for the strongest peaks of respective synthesized NPs.

Table 2: The calculated parameters for the major peaks of Ag NPs

2θ	θ	B	D(nm)	D average(nm)	d-spacing	δ x10^3(nm^{-2})
38.14	19.07	0.66	12.75	12.62	2.36	6.15
44.20	22.10	1.25	6.84		2.05	21.37
64.50	32.25	0.58	16.04		1.44	3.88
77.40	38.70	0.686	14.84		1.23	4.54

The average crystallite size of the Ag NPs NPs was deduced to be 12.62 nm

Table 3: The calculated parameters for the major peaks of Co_3O_4 NPs

2θ	θ	β	D(nm)	D average (nm)	d-spacing	δ x10^3(nm^{-2})
19.19	9.60	0.65	12.49	12.75	4.62	6.41
31.47	15.74	0.64	12.87		2.84	6.04
37.00	18.50	0.66	12.70		2.43	6.20
38.73	19.37	0.76	11.08		2.32	8.14
44.96	22.48	0.71	12.05		2.02	6.88
55.74	27.87	0.66	13.62		1.65	5.40
59.45	29.72	0.82	11.19		1.55	7.99
65.34	32.67	0.78	12.02		1.43	6.92
77.42	38.71	0.61	16.69		1.23	3.59

The average crystallite size of the Co_3O_4 NPs was deduced to be 12.75 nm.

Table 4: The calculated parameters for the major peaks of Ag/Co_3O_4 BMNPs

2θ	θ	β	D(nm)	D (average (nm)	d-spacing	δ x10^3(nm^{-2})
31.34	15.67	0.55	15.09	18.07	2.85	4.39
36.92	18.46	0.66	12.61		2.43	6.29
38.20	19.10	0.38	22.12		2.35	2.05
44.38	22.19	0.51	16.70		2.04	3.59
59.36	29.68	0.56	16.33		1.55	3.75
64.54	32.27	0.50	18.88		1.40	2.81
77.44	38.72	0.41	24.77		1.23	1.63

The average crystallite size of the Ag/Co_3O_4 BMNPs was deduced to be 18.07 nm.

Dislocation density measures the number of dislocations in a unit volume of crystalline materials. Thus, as the particle size of nanoparticles increases the dislocation density of the crystalline materials is decreased. The synthesized Ag NPs, Co_3O_4 NPs and Ag/Co_3O_4 BMNPs an average crystalline size of 12.62 nm, 12.75 nm and 18.07 nm respectively and peak position (2θ) are increased in these sequences. Since dislocation density depends upon particle size that means as particle size increases dislocation density decreases. Thus, the dislocation density decreases in the order of Ag NPs < Co_3O_4 < Ag/Co_3O_4 BMNPs.

4.3. UV- Vis spectroscopy analysis

The optical properties of the synthesized Ag NPs Co_3O_4 NPs and Ag/Co_3O_4 BMNPs are presented as follows. Figure 8 (a and b) showed the absorption spectra and energy band gap for Ag NPs. Figure 9 (a and b) below depicted the absorption spectra, and energy band gap for Co_3O_4 NPs and figure 10 (a and b) below depicted the absorption spectra, and energy band gap for Ag/Co_3O_4 BMNPs respectively.

For synthesized Ag NPs the absorption bands was observed at 402 nm as shown in Figure 8 (a). The result revealed that the formation of silver nanoparticles by exhibiting the typical surface plasmon resonance absorption. This surface plasmon resonance property of metal nanoparticle is due to the combined vibration of free electrons in resonance with light wave (Das et al., 2016). In the parabolic band structure, the band gap energy, Eg and the absorption coefficient of a direct band gap semiconductor are related through Equation (3):

$$(\alpha h\nu)2 = A(h\nu - Eg) \quad (3)$$

Where, ħ is Planck's constant, ν is the photon's frequency, and A is the slope in the linear region. Taking the K–M scattering coefficient S as a constant concerning the wavelength, and using the remission function in equation (2), the following expression was derived Equation (4):

$$(F(R)h\nu)2 = A(h\nu - Eg) \quad (4)$$

Where, F(R) is equal to K/S, the molar absorption coefficient K is equal to $(1 - R)^2$, the scattering factor S is equal to 2R, and R is the reflectance of the materials and is defined as $\frac{\%R}{100}$. The direct and indirect bandgap energies of the nanomaterials were determined by extrapolation of the linear portion of Kubelka–Munk (K–M) plots (Abebe et al., 2020).

The bandgap energy for the synthesized silver nanoparticles was determined by the Tauc relations which are discussed in equation (4) and the plots were shown in figure 8 (b), which indicates band gap of synthesized silver nanoparticles are 3.38 eV.

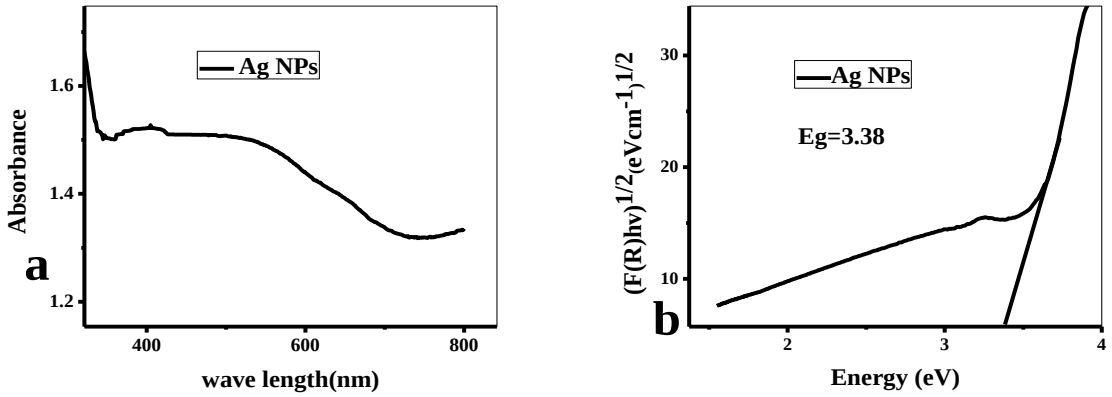

Figure 8: (a) Wavelength versus Absorbance of UV-Vis spectroscopy, (b) energy versus band gap of Ag NPs.

The absorption band of light in metal nanoparticle is defined as intra-band gap excitation of conduction electrons from the lowest energy state to higher energy states near the Fermi level of the conduction band upon receiving photon energy having the maximum absorbance wavelength (λ_{max}). A smaller particle size has fewer atoms and can potentially have less of an attraction between its metal ions and conduction electrons. As a result, the particle's conduction band energy rises. However, because larger particles have more atoms, there is a

greater potential for attraction between conduction electrons and metal ions, which lowers the conduction band energy of the metal nanoparticles (Shrestha & Adhikari, 2017).

The absorption spectra and energy band gap of Co_3O_4 NPs and Ag/Co_3O_4 BMNPs are shown Figure 9 (a and b) and Figure 10 (a and b) respectively.

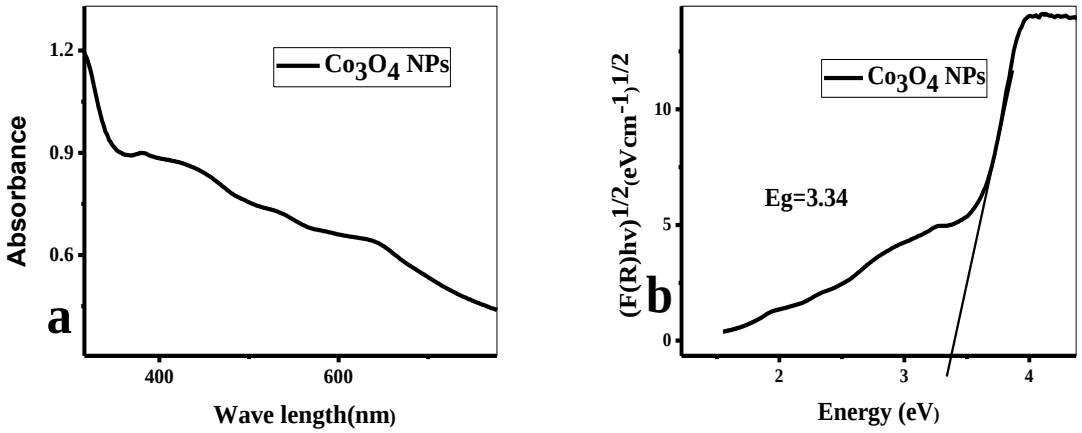

Figure 9: (a) Wavelength versus Absorbance of UV-Vis spectroscopy, (b) energy versus band gap of Co_3O_4 NPs.

Two different oxidation states persist in the cobalt (Co^{3+} and Co^{2+}) ion which may be the reason for the existence of two absorption peaks in the UV-Vis spectroscopy. The formation of absorption bands was caused by the charge transfer processes from O^{2-} to Co^{2+} and O^{2}- to Co^{3+}, which results in larger band gap and lower band gap energies, respectively. The two absorption peak observed between 500-580 nm and 600-680 nm respectively for Co_3O_4 nanoparticles, were in good agreement with the previous reports (B. Vennela, 2019). As in Eltarahony et al. the first band can be assigned to the $O^{2-} \rightarrow Co^{2+}$ charge transfer process and the second one to the $O^{2-} \rightarrow Co^{3+}$ charge transfer, which suggested formation of cobalt oxide. As illustrated in Figure 9 (a), a surface plasmon absorption peak (SPR) was observed at wavelengths 400–450 nm. The SPR phenomenon arises due to the metallic NPs physically absorbed light, and as a result of this absorption, conduction electrons of metal undertake coherent oscillation (Eltarahony et al., 2018).

The energy band gap of Co_3O_4 NPs was found to be 3.34 eV, as shown in figure 9(b), due to the electron creates holes in the valence band to the conduction band. The optical band gap energy increases the potential well of small lateral dimensions of cobalt oxide nanoparticle

due to quantum confinement effect. The positive holes exchange between Co^{3+} and Co^{2+} transfer of O^{2-} between filled sides with vacant oxygen side (Agilandeswari & Rubankumar, 2015).

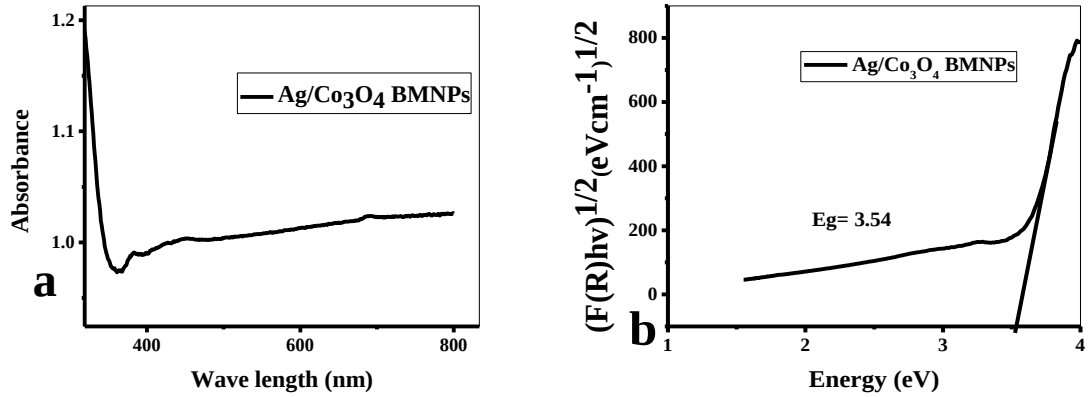

Figure 10: (a) Wavelength versus Absorbance of UV-Vis spectroscopy, (b) energy versus band gap of Ag/Co_3O_4 BMNPs.

From Figure 10 (b) the optical energy band gap of Ag/Co_3O_4 BMNPs found to be 3.54 eV. The optical band gap increased on average in the final BMNPs relative to their monometallic counterpart. This indicates that the BMNPs exhibited strong quantum confinement, which shifts the energy levels of the conduction and valence bands apart and gives rise to a blue shift in the transition energy as the particle size decreases (Fredrick & Mangaka, 2017).

4.4. Scanning Electron Microscopy (SEM) analysis

The morphology and texture of the synthesized Ag NPs, Co_3O_4 NPs and Ag/Co_3O_4 BMNPs as depicted by SEM micrographs are shown in Figures 11 (a), 11(b) and 11(c) respectively. The SEM image of the synthesized Ag NPs was shown in Figure 11 (a). The SEM micrograph demonstrates that the Ag NPs agglomerated to form either clusters or large nanoparticle. This agglomeration is due to the narrow distance between surfaces of nanoparticles caused by the attractive van der waals force and/or the driving force that tends to minimize the total surface energy of the system (Shameli et al., 2015). The SEM images of Co_3O_4 NPs Figure 11(b) demonstrated the nonhomogeneity of the particles in terms of their shape and size. The micrographs show that the Co_3O_4 NPs were found to possess spherical as well as irregular geometries of Co_3O_4 NPs with varying particle sizes were found in the micrographs. Ag/Co_3O_4 BMNPs SEM micrograph Figure 11(c) also showed the nonhomogeneity of the particles in

terms of their shape and size. The micrographs show that the Ag/Co_3O_4 BMNPs were found to possess spherical as well as irregular geometries of Ag/Co_3O_4 BMNPs with varying particle sizes were found in the micrographs.

.

a) 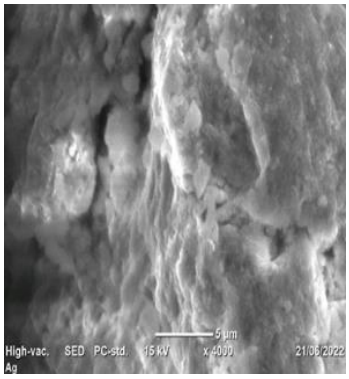 b) 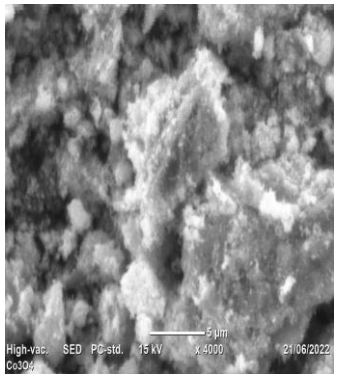 c) 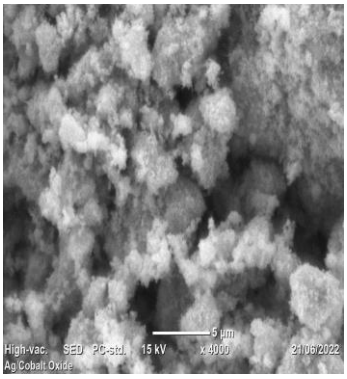

Figure 11: SEM image of (a) Ag NPs (b) Co_3O_4 NPs (c) Ag/Co_3O_4 BMNPs

4.5. Fourier Transform Infrared (FT-IR) Spectroscopy analysis

FTIR analysis for the green synthesized, Ag NPs, Co_3O_4 NPs and Ag/Co_3O_4 BMNPs and the leaf extract of *Croton macrostachyus* were carried out in order to explore the formation of Ag NPs, Co_3O_4 NPs and Ag/Co_3O_4 BMNPs and confirm the functional groups present in the leaf extract of *Croton macrostachyus* plant. This is used to identify the possible bioactive molecules which were actively involved during the synthesis process as stabilizing and capping agents to prevent the overall growth of Ag NPs, Co_3O_4 NPs and Ag/Co_3O_4 BMNPs. Figure 12 showed the FT-IR result of leaf extract of *Croton macrostachyus* plant and Ag NPs. The FTIR spectrum for leaf extract of *Croton macrostachyus* plant figure 12(a) showed the absorption bands at 3431 cm^{-1}, 2921 cm^{-1}, 2114 cm^{-1}, 1631 cm^{-1}, 1455 cm^{-1}, 1027 cm^{-1} and 543 cm^{-1}. The broad peak observed in the spectrum at around 3431 cm^{-1} confirming the presence of O-H stretching. While, the absorption peak located at around 2921 cm^{-1} reveal the presence of C-H stretching vibrations of alkane. The peak observed around 2114 cm^{-1} represents the nitrile (C ≡ N) functional groups. A peak at 1631 cm^{-1} showed the presence amide (C=O) stretch and the observed peak at 1455 cm^{-1} showed N-H Bend of primary amines and C-H alkanes Bending. The absorptions peak around 1027 cm^{-1} C-O stretch of ether functional group. The peak at 543 cm^{-1} may corresponds to the presence of aryl disulfide (S–S) or Polysulfides (S–S stretch) or C–Br stretch.

However, for the synthesized Ag NPs, the FTIR spectrum exhibited some shifting of the peaks; peak intensity decreased/increased, and disappeared, as observed in Figure (b). The peak shifted, suggesting that the responsible functional groups were involved in the binding mechanism on the Ag NPs. After the synthesis process, the peaks at 3431 cm^{-1}, 2921 cm^{-1}, 1631 cm^{-1}, 1455 cm^{-1}, 1027 cm^{-1} and 543 cm^{-1} shifted to 3395 cm^{-1}, 2911 cm^{-1}, 1597 cm^{-1}, 1344 cm^{-1} and 1005 cm^{-1}, 3395 cm^{-1} corresponding to –OH stretching of the carboxylic acid. The peak absorption at 2911 cm^{-1} corresponds to C-H stretching of Alkane. While, the peak at 1597 cm^{-1}, 1344 cm^{-1} indicates N=O Stretch of the Nitro Groups and N=O Bend of the nitro group. The absorption peak at 1005 cm^{-1} indicated C-O stretch of ether functional group respectively (Farsi & Farokhi, 2018; Sharma et al., 2022; Teshale et al., 2020).

The FTIR spectrum of Co_3O_4 NPs and Ag/Co_3O_4 BMNPs also showed some shifting of the peaks; peak intensity decreased/increased, and disappeared. Figure 13 showed the FT-IR results of Co_3O_4 NPs and Ag/Co_3O_4 BMNPs. The absorption peaks of Co_3O_4 NPs and Ag/Co_3O_4 BMNPs were observed at 3391 cm^{-1}, 2920 cm^{-1}, 2356, 2060, 1618, 1349 cm^{-1}, 1046 cm^{-1}, 825 cm^{-1} and 3324 cm^{-1}, 2921 cm^{-1}, 2356 cm^{-1}, 2080 cm^{-1}, 1550 cm^{-1}, 1362 cm^{-1}, 1013 cm^{-1}, 799 cm^{-1}, 666 cm^{-1}, 570 cm^{-1} respectively.

Figure 13(a) indicates the FT-IR spectra of the sample Co_3O_4 NPs exhibits, the absorption peak at 3391 corresponding to –OH stretching of the carboxylic acid. The absorption peak located at around 2921 cm^{-1} reveal the presence of C-H stretching vibrations of alkane. While, the peak observed around 2080 cm^{-1} represents the nitrile (C ≡ N) functional groups. The peaks located at 1618 cm^{-1} may be due to C=C stretching. 1349 cm^{-1} and 1046 cm^{-1} corresponding to N=O Bend of the nitro group and C-O stretch of ether functional group respectively. The absorption peak observed at 577 cm^{-1} corresponds to the stretch Co-O present in cobalt oxide nanoparticles.

Figure 13(b) shows FT-IR spectra of the sample Ag/Co_3O_4 BMNPs exhibits, band at the band at 3324 cm-1 indicated the –OH stretching of the carboxylic acid. The band located at around 2921 cm^{-1} shows the presence of C-H stretching vibrations of alkane. The absorption peak around 1550 cm^{-1} and 1362 cm^{-1} indicated N=O Stretch of the Nitro Group and N=O Bend of the nitro group. While, the absorption peak at 1013 cm^{-1} indicated the presence of C-O stretch of ether functional group. The absorption peak at 666 cm^{-1} corresponds to the stretch vibrations of the O-Co-O and 570 cm^{-1} corresponds to the stretch Co-O present in Ag/Co_3O_4

BMNPs. The peak at 799 cm^{-1} may corresponds to the presence substituted alkene (Asha et al., 2022; Bekele et al., 2022; Kainat et al., 2021; Teshale et al., 202).

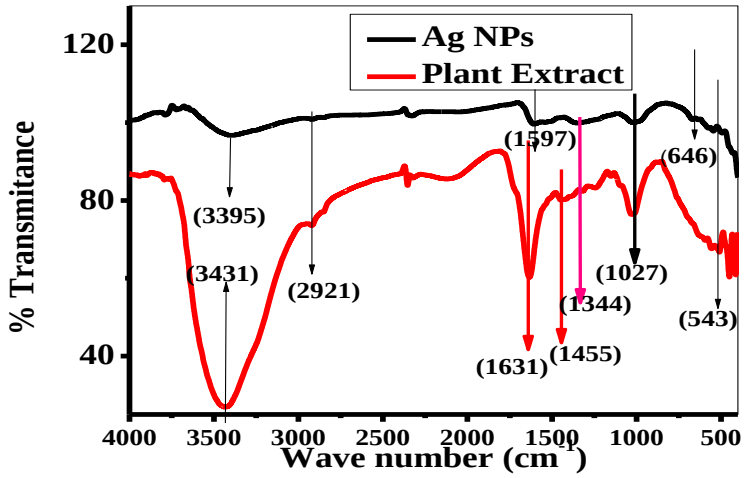

Figure 12: FTIR spectra of (a) *Croton macrostachyus* plant extract, (b) Ag NPs

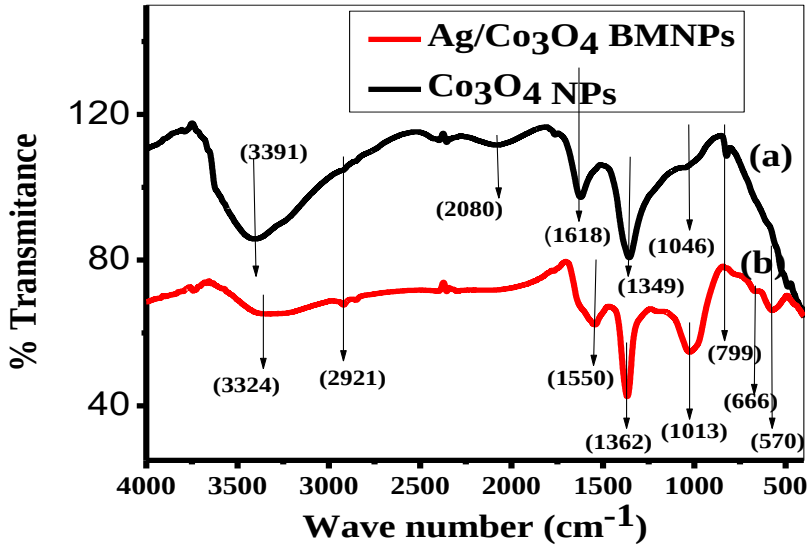

Figure 13: FTIR spectra of (a) Co_3O_4 NPs, (b) Ag/Co_3O_4 BMNPs

4.6. Thermogravimetric/differential thermal analysis (TGA/DTA) analysis

The thermal behaviour or thermal stability of biosynthesized Co_3O_4 NPs and Ag/Co_3O_4 BMNPs that were capped by phytochemicals of *Croton macrostachyus* plant extract was investigated via thermogravimetric analysis. Thermogravimetric analysis was conducted under a nitrogen atmosphere at a heating rate of 10 C/min, and the weight loss process was observed in two steps as revealed from the TGA-DTG curves. For Co_3O_4 NPs weight loss of 81.66% was observed from room temperature to 348 ^oC. The first 30.41% could be due to the loss of residual ethanol or absorbed moisture. The second weight loss 51.25% could be due to the loss of oxygen, enhancing the formation of oxygen vacancies. The weight loss is due to thermal decomposition or dehydration of Co_2O_4 to Co_3O_4 particles. For Ag/Co_3O_4 BMNPs weight loss of 10.1% was observed from room temperature to 467 ^oC. The first 3.5% could be due to the loss of residual ethanol or absorbed moisture. The corresponding DTA showed two endothermic peaks at the same temperatures. According to the TGA/DTA analysis, the total weight loss of the biosynthesized Co_3O_4 NPs and Ag/Co_3O_4 BMNPs were approximately 81.66% and 10.1% respectively which supports the capping of s Co_3O_4 NPs and Ag/Co_3O_4 BMNPs by *Croton macrostachyus* extract phytochemicals.

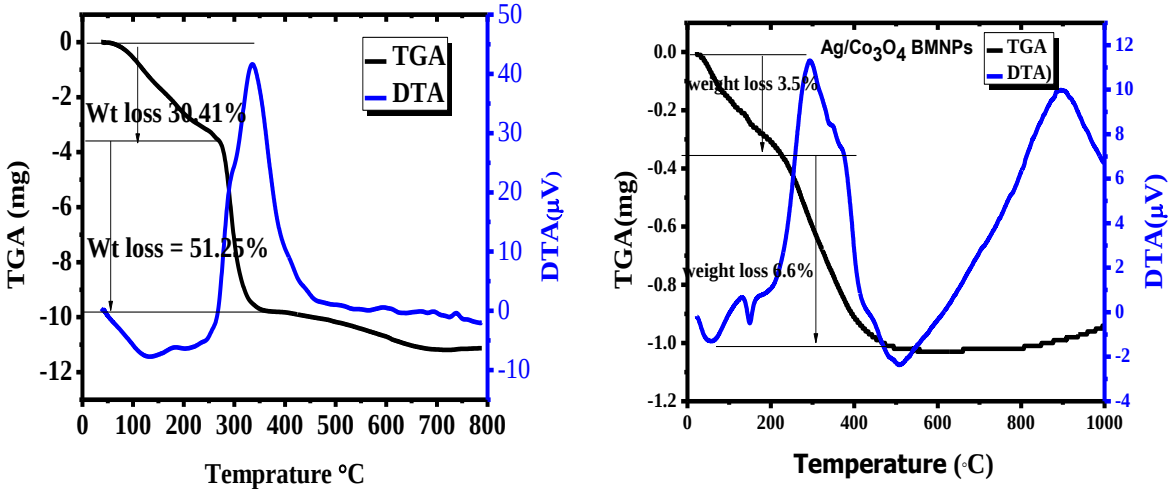

Figure 14: TGA and DTA results of a) Co_3O_4 NPs and b) Ag/Co_3O_4

4.7. Antibacterial activity of synthesized Ag NPs, Co_3O_4 NPs and Ag/ Co_3O_4 BMNPs

In this section, the antibacterial activities of the synthesized NPs were discussed. The antibacterial activity of *Croton macrostachyus* leaf extract templated synthesized Ag NPs, Co_3O_4 NPs and Ag/Co_3O_4 BMNPs were investigated via the method of agar disc diffusion

assay. (Figure 15, 16 and 17) indicates the antibacterial activity of the synthesized Ag NPs, Co_3O_4 NPs and Ag/Co_3O_4 BMNPs against the bacterial strains gram-negative *Escherichia-coli* and *Salmonella typhimirium* and gram-positive *Staphylococcus aureus and Enterococcus faecalis* respectively.

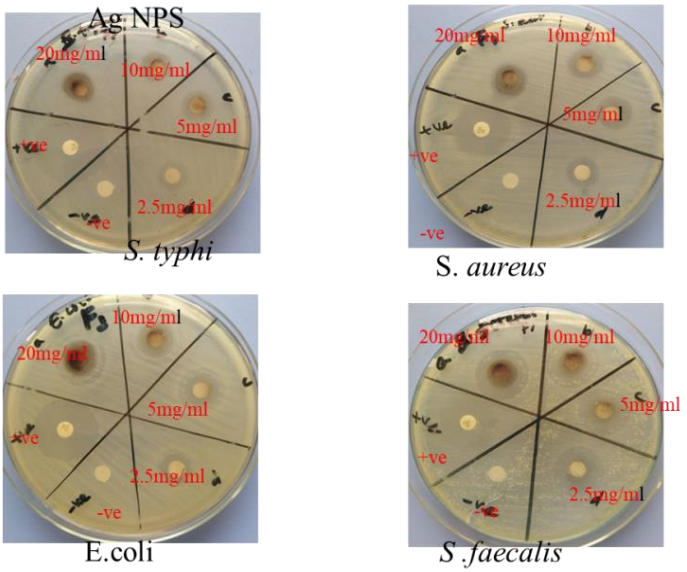

Figure 15: Antibacterial activities of Ag NPs against *Escherichia-coli, Salmonella typhimurium, Staphylococcus aureus and Enterococcus faecalis*.

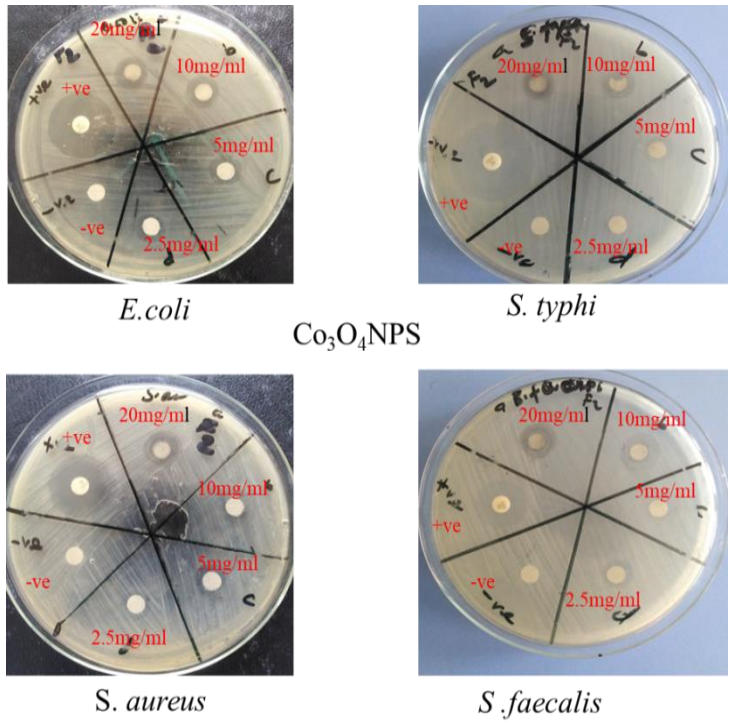

Figure 16: Antibacterial activities of Co_3O_4NPs against *Escherichia-coli Salmonella typhimurium, Staphylococcus aureus* and *Enterococcus faecalis*.

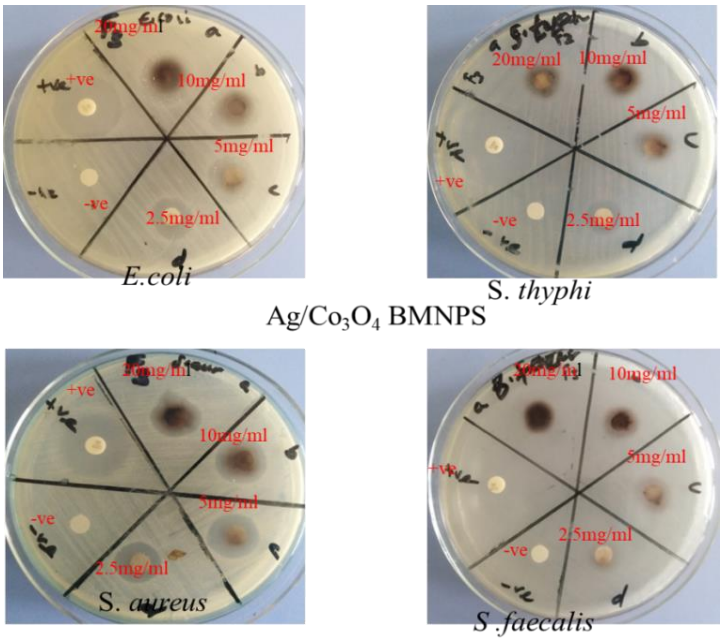

Figure 17: Antibacterial activities of Ag/Co_3O_4 BMNPs against *Escherichia-coli, Salmonella typhimurium, Staphylococcus aureus and Enterococcus faecalis*.

The antibacterial activity of the synthesized Ag NPs, Co_3O_4 NPs and Ag/Co_3O_4 BMNPs against the bacterial strains gram-negative *Escherichia-coli* and *Escherichia-coli, Salmonella typhimurium* and gram-positive *Staphylococcus aureus and Enterococcus faecalis* were tabulated and discussed in the tables (5, 6. and 7) respectively.

Table 5: Zones of inhibition of Ag NPs and Contrimoxazole (+ve control) with different concentrations against different bacterial strains.

sample	Concentration (mg/ml)	Zone of inhibition (mm).			
		Gram-negative species		Gram-positive species	
		Escherichia-coli ATCC25922	*Salmonella typhimurium* ATCC13311	*Staphylococcus aureus* ATCC25923	*Enterococcus faecalis* ATCC29212
Ag NPs	20	16.167 ± 0.167	14.33 ± 0.167	14.167 ± 0.167	21.33 ± 0.33
	10	15 ± 0.2887	13.167 ± 0.167	12.83 ± 0.441	19.3 ± 0.33
	5	12 ± 0.2887	12 ± 0.2887	12.167 ± 0.167	18.33 ± 0.33
	2.5	11.167 ± 0.167	10.33 ± 0.167	10.33 ± 0.167	17.167 ± 0.167
Contrimoxazole (+ve) control		22.83 ± 0.167	23.83 ± 0.167	22	22.167 ± 0.167
DMSO (-ve) control		6	6	6	6

Table 6: Zones of inhibition of Co_3O_4 NPs and Contrimoxazole (+ve control) with different concentrations against different bacterial strains.

sample	Concentration (mg/ml)	Zone of inhibition (mm)			
		Gram-negative species		Gram-positive species	
		Escherichia-coli ATCC25922	*Salmonella typhimurium* ATCC13311	*Staphylococcus aureus* ATCC25923	*Enterococcus faecalis* ATCC29212
Co_3O_4 NPs	20	12.33 ± 0.33	11.83 ± 0.167	10.5 ± 0.2887	12 ± 0.2887
	10	10	9	9 ± 0.5	11 ± 1
	5	9.167 ± 0.167	8.167 ± 0.167	7.667 ± 0.167	8.83 ± 0.167
	2.5	8 ± 0.2887	6	7.167 ± 0.167	7.33 ± 0.167
Contrimoxazole (+ve) control		23	23.833 ± 0.167	22.167 ± 0.167	18
DMSO (-ve) control		6	6	6	6

Table 7: Zones of inhibition of Ag/Co_3O_4 BMNPs and Contrimoxazole (+ve control) with different concentrations against different bacterial strains.

sample	Concentration (mg/ml)	Zone of inhibition (mm)			
		Gram-negative species		Gram-positive species	
		Escherichia-coli ATCC25922	*Salmonella typhimurium* ATCC13311	*Staphylococcus aureus* ATCC25923	*Enterococcus faecalis* ATCC29212
Ag/Co_3O_4 BMNPs	20	17.5 ± 0.2887	13.5 ± 0.2887	15.5	12 ± 0.577
	10	16.167 ± 0.167	12.33 ± 0.33	15.167 ± 0.167	11 ± 0.577
	5	14.167 ± 0.167	12.5 ± 0.2887	14.167 ± 0.167	9.33 ± 0.33
	2.5	12.167 ± 0.167	11.167 ± 0.167	13 ± 0.2887	7.833 ± 0.440
Contrimoxazole (+ve) control		22.167 ± 0.167	21.167 ± 0.167	24.833 ± 0.167	21.833 ± 0.167
DMSO (-ve) control		6	6	6	6

As shown in figure 18 supported by table (5-6), the antibacterial activity of the synthesized Ag NPs, Co_3O_4 NPs and Ag/Co_3O_4 BMNPs were enhanced with increasing the concentration of the nanoparticles. The presence of an inhibition zone indicates that the mechanism of the biocidal action of synthesized nanoparticles involves disruption of the cell membrane of bacterial species and finally leads to the death of pathogens. Thus, the size of the inhibition zone was different according to the type of pathogens, the concentration of the synthesized nanoparticles and the types of nanoparticles.

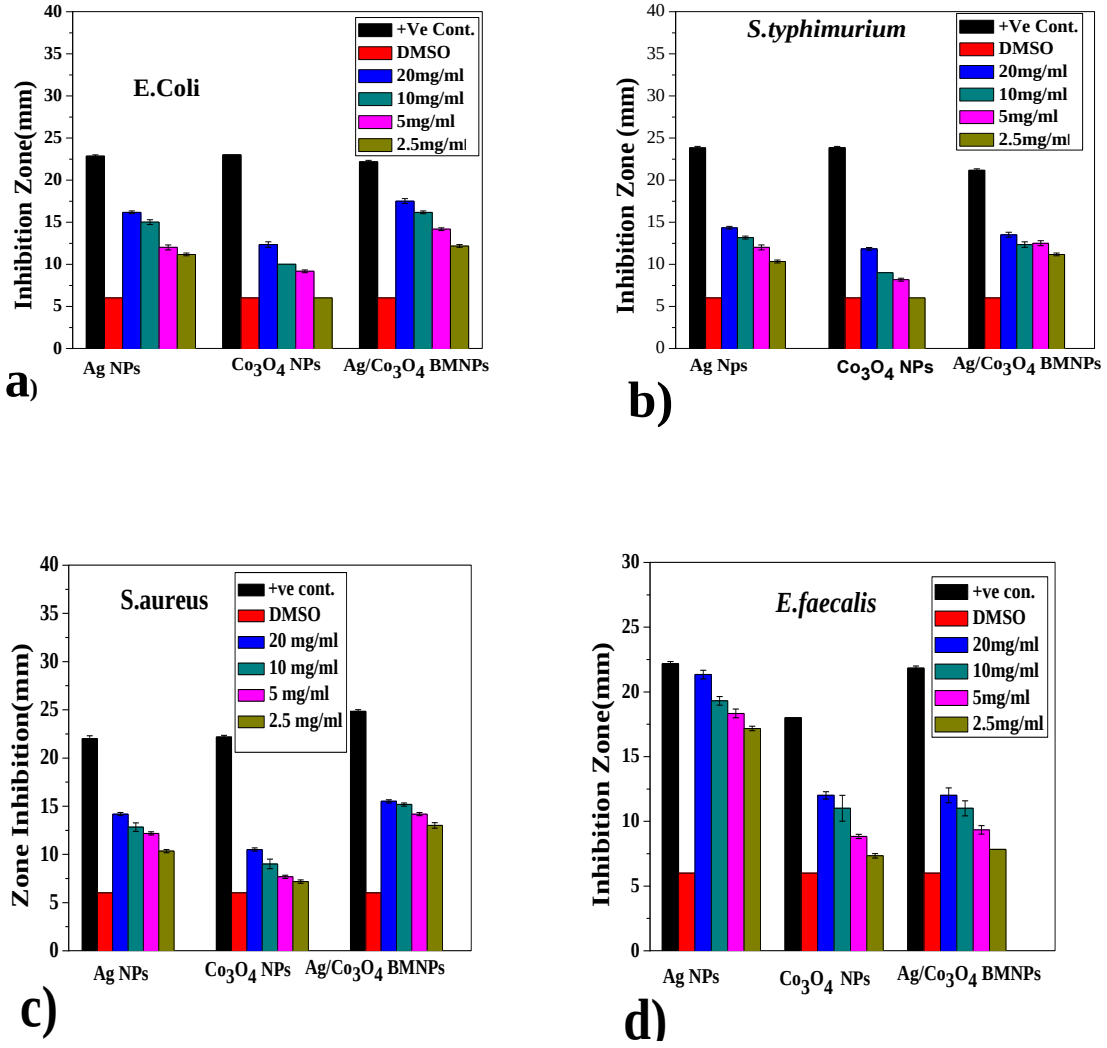

Figure 18: Inhibition Zone of Ag NPs, Co_3O_4 NPs and Ag/Co_3O_4 BMNPs *Escherichia-coli, Salmonella typhimurium, Staphylococcus aureus,* and *Enterococcus faecalis.*

When the anti-bacterial activity of synthesized Ag NPs, Co_3O_4 NPs and Ag/Co_3O_4 BMNPs compared to each other against selected bacterial strains *Escherichia-coli, Salmonella typhimurium, Staphylococcus aureus* and *Enterococcus faecalis),* Ag/Co_3O_4 BMNPs exhibited best inhibition activities toward the selected bacterial species (*Escherichia-coli* and *Staphylococcus aureus*) than that of Ag NPs and Co_3O_4NPs inhibition activities. However, Ag NPs exhibited best inhibition activities toward *Salmonella typhimurium* and *Enterococcus faecalis* bacteria species. Co_3O_4 NPs showed least inhibition activities against selected bacterial species compared to Ag NPs and Ag/Co_3O_4 BMNPs. Ag NPs target both the respiratory chain and the cell-division machinery, while concomitantly releasing silver ions

(Ag^{+}) that increase bactericidal activity and finally leading to cell death (Padilla-Cruz et al., 2021). For cobalt oxide NPs, the different positive states of cobalt ions, i.e., Co^{2+} and Co^{3+} interact with the parts of the bacterial cell that have a negative charge and cause the death of the bacterial cell. Second, there may be the excitement of electrons on the surface of cobalt oxide because of light irradiation in the conduction and valence band. In the conduction band, there is the formation of superoxide radical anion because of the reaction of excited electrons and oxygen molecules. Finally, the formation of hydrogen peroxide, which is a strong oxidant, occurs. On the surface of NPs, the reaction of water and superoxide radical anion destroys the bacterial cell (Iravani & Varma, 2020).

5. CONCLUSION AND RECOMMENDATION

5.1. Conclusion

In the present findings, Ag NPs, Co_3O_4 NPs and Ag/Co_3O_4 BMNPs were synthesized via the green synthesis method by using *Croton macrostachyus* leaf extract. The green-synthesized Ag NPs, Co_3O_4 NPs and Ag/Co_3O_4 BMNPs were characterized using XRD, UV-DRS, SEM, FTIR, and TGA. The XRD analysis reveals the average crystallite sizes of 12.62 nm, 12.746 nm, and 18.07nm for the synthesized Ag NPs, Co_3O_4 NPs and Ag/Co_3O_4 BMNPs, respectively. The UV-DRS result suggests the energy band gap for synthesized Ag NPs, Co_3O_4 NPs and Ag/Co_3O_4 BMNPs were deduced to be 3.38 eV, 3.34 eV and 3.54 eV, respectively. The SEM images showed clusters or large nanoparticles for Ag NPs and spherical as well as irregular geometries which is nonhomogeneity of the particles in terms of their shape and size for Co_3O_4 NPs and Ag/Co_3O_4 BMNPs. The antibacterial activity of the green synthesized Ag NPs, Co_3O_4 NPs and Ag/Co_3O_4 BMNP NPs was evaluated against Escherichia-*coli, Salmonella typhimurium, Staphylococcus aureus and Enterococcus faecalis*. Ag/Co_3O_4 BMNPs showed enhanced activities toward (*Escherichia-coli* and *Staphylococcus aureus*) than that of Ag NPs and Co_3O_4 NPs inhibition activities. However, Ag NPs showed enhanced activities toward *Escherichia-coli, Salmonella typhimurium* and *Enterococcus faecalis* bacteria species. Co_3O_4 NPs showed least inhibition activities against selected bacterial species compared to Ag NPs and Ag/Co_3O_4 BMNPs.

5.2.Recommendation

Bimetallic nanoparticle synthesis through green methods is one of the emerging research areas with huge future prospective. Thus, further studies may be required for the synthesis of Ag/Co_3O_4 BMNPs and their applications such as in the field of optoelectronic devices, catalysis and biomedical applications. And also I recommend the synthesized nanoparticles need further characterization by different instruments like EDX, TEM, HRTEM, DLS and SAED analysis.

Research Fund Acknowledgment

This work is financially supported by Adama Science and Technology University and the Ministry of Innovation and Technology of Ethiopia under the grant number **ASTU/SMR/253/21**, Adama, Ethiopia.

REFERENCE

Aazam, E. S., & Zaheer, Z. (2022), 'Silver-Cobalt bimetallic nanoparticles to the generation of hydrogen from formic acid decomposition,' *Arabian Journal of Chemistry*, *15*(5).

Abbasi, E., Aval, S. F., Akbarzadeh, A., Milani, M., Nasrabadi, H. T., Joo, S. W., Hanifehpour, Y., Nejati-Koshki, K., & Pashaei-Asl, R. (2014), 'Dendrimers: synthesis, applications, and properties,' *Nanoscale Research Letters*, *9*(1).

Abebe, B., Murthy, H. C. A., Zereffa, E. A., & Adimasu, Y. (2020), 'Synthesis and characterization of ZnO/PVA nanocomposites for antibacterial and electrochemical applications,' *Inorganic and Nano-Metal Chemistry*, *51*(8).

Abou El-Nour, K. M., Eftaiha, A., Al-Warthan, A., & Ammar, R. A. (2010), 'Synthesis and applications of silver nanoparticles,' *Arabian Journal of Chemistry*, *3*(3): pp. 135–140.

Adam, F., Chew, T. S., & Andas, J. (2011), 'A simple template-free sol–gel synthesis of spherical nanosilica from agricultural biomass,' *Journal of Sol-Gel Science and Technology*, *59*(3).

Adetunji, C. O., Olaniyi, O. O., & Ogunkunle, A. T. J. (2013), 'Bacterial activity of crude extracts of Vernonia amygdalina on clinical isolates', *Journal of Microbiology and Antimicrobials*, *5*(6).

Aga, W. S., Fantaye, S. K., & Jabasingh, S. A. (2020), 'Biodiesel production from Ethiopian 'Besana'- Croton macrostachyus seed: Characterization and optimization,' *Renewable Energy*, *157*.

Agilandeswari, K., & Rubankumar, A. (2015), 'Synthesis, Characterization, Optical, and Magnetic Properties of Co_3O_4 Nanoparticles by Quick Precipitation,' *Synthesis and Reactivity in Inorganic, Metal-Organic, and Nano-Metal Chemistry*, *46*(4): pp. 502–506.

Ahmad, N., Sharma, S., Alam, M. K., Singh, V., Shamsi, S., Mehta, B., & Fatma, A. (2010), 'Rapid synthesis of silver nanoparticles using dried medicinal plant of basil,' *Colloids and Surfaces B: Biointerfaces*, *81*(1).

Ahmed, S., Ahmad, M., Swami, B. L., & Ikram, S. (2016), 'A review on plants extract mediated synthesis of silver nanoparticles for antimicrobial applications: A green expertise,' *Journal of Advanced Research*, *7*(1).

Ai, L., Liu, X., & Jiang, J. (2015), 'Synthesis of loofah sponge carbon supported bimetallic silver–cobalt nanoparticles with enhanced catalytic activity towards hydrogen generation from sodium borohydride hydrolysis,' *Journal of Alloys and Compounds, 625.*

Akinsiku, A. A., Dare, E. O., Ajani, O. O., Ayo-Ajayi, J., Ademosun, O. T., & Ajayi, S. O. (2018), 'Room temperature Phytosynthesis of Ag/Co bimetallic nanoparticles using aqueous leaf extract of *Canna indica*,' *IOP Conference Series: Earth and Environmental Science, 173.*

Ali Dheyab, M., Abdul Aziz, A., Jameel, M. S., Moradi Khaniabadi, P., & Oglat, A. A. (2020), 'Rapid Sonochemically-Assisted Synthesis of Highly Stable Gold Nanoparticles as Computed Tomography Contrast Agents,' *Applied Sciences, 10*(20).

Ali Dheyab, M., Aziz, A. A., & Jameel, M. S. (2021), 'Recent Advances in Inorganic Nanomaterials Synthesis Using Sonochemistry: A Comprehensive Review on Iron Oxide, Gold and Iron Oxide Coated Gold Nanoparticles,' *Molecules, 26*(9).

Alvi, G. B., Iqbal, M. S., Ghaith, M. M. S., Haseeb, A., Ahmed, B., & Qadir, M. I. (2021), 'Biogenic selenium nanoparticles (SeNPs) from citrus fruit have anti-bacterial activities,' *Scientific Reports, 11*(1).

Ansari, S., Bhor, R., Pai, K., Sen, D., Mazumder, S., Ghosh, K., Kolekar, Y., & Ramana, C. (2017), 'Cobalt nanoparticles for biomedical applications: Facile synthesis, physiochemical characterization, cytotoxicity behavior and biocompatibility,' *Applied Surface Science, 414.*

Anu Mary Ealia, S., & Saravanakumar, M. P. (2017), 'A review on the classification, characterisation, synthesis of nanoparticles and their application,' *IOP Conference Series: Materials Science and Engineering, 263.*

Asha, G., Rajeshwari, V., Stephen, G., Gurusamy, S., & Carolin Jeniba Rachel, D. (2022), 'Eco-friendly synthesis and characterization of cobalt oxide nanoparticles by sativum species and its photo-catalytic activity,' *Materials Today: Proceedings, 48.*

Ashok, A., Kumar, A., & Tarlochan, F. (2018), 'Surface Alloying in Silver-Cobalt through a Second Wave Solution Combustion Synthesis Technique,' *Nanomaterials, 8*(8): pp. 604.

B. Vennela, A. (2019), ‘Structural and Optical Properties of Co3O4 Nanoparticles Prepared by Sol-gel Technique for Photocatalytic Application,’ *International Journal of Electrochemical Science*.

Banne, S. V., Patil, M., Kulkarni, R., & Patil, S. (2017), ‘Synthesis and Characterization of Silver Nano Particles for EDM Applications,’ *Materials Today: Proceedings*, *4*(11).

Bekele, E. T., Murthy, H. C. A., Muniswamy, D., Lemenh, Y. A., Shume, M. S., Tadesse Ayanie, G., Kumar, A. P., Ravikumar, C. R., Balachandran, R., & Roy, A. (2022), ‘Solanum tuberosum Leaf Extract Templated Synthesis of Co_3O_4 Nanoparticles for Electrochemical Sensor and Antibacterial Applications,’ *Bioinorganic Chemistry and Applications*.

Bindhu, M., & Umadevi, M. (2015), ‘Antibacterial and catalytic activities of green synthesized silver nanoparticles,’ *Spectrochimica Acta Part A: Molecular and Biomolecular Spectroscopy*, *135*.

Bokov, D., Turki Jalil, A., Chupradit, S., Suksatan, W., Javed Ansari, M., Shewael, I. H., Valiev, G. H., & Kianfar, E. (2021), ‘Nanomaterial by Sol-Gel Method: Synthesis and Application. *Advances in Materials Science and Engineering*.

Boroujeni, K. P., Shahrokh, M., Karvani, J., Moradi, N., Farokhnia, A., & Mobini, M. (2019), ‘Synthesis and Study of Catalytic, Anti–Bacterial, Anti–Oxidant, and DNA Cleavage Properties of Ag–Co and Ag–Ni Magnetic Nanoparticles,’ *Acta Chimica Slovenica*, *66*(3).

Boverhof, D. R., Bramante, C. M., Butala, J. H., Clancy, S. F., Lafranconi, M., West, J., & Gordon, S. C. (2015), ‘Comparative assessment of nanomaterial definitions and safety evaluation considerations,’ *Regulatory Toxicology and Pharmacology*, *73*(1).

Bowman, D. M. (2017), ‘More than a Decade On: Mapping Today’s Regulatory and Policy Landscapes Following the Publication of Nanoscience and Nanotechnologies: Opportunities and Uncertainties,’ *NanoEthics*, *11*(2).

Camargo, P. H. C., Satyanarayana, K. G., & Wypych, F. (2009), ‘Nanocomposites: synthesis, structure, properties and new application opportunities,’ *Materials Research*, *12*(1).

Chang, W., Skandan, G., Hahn, H., Danforth, S. C., & Kear, B. (1994), ‘Chemical Vapor Synthesis of Nanostructured Ceramics,’ *MRS Proceedings*, *351*.

Chiang, I. D. N. K., Lim, M. S. S., & Peng, D. C. (2014), 'Novel Bimetallic Tin-Manganese Oxides/Carbon Nanotube Nanocomposite and Their Charge Storage Properties,' *the Journal of the Institution of Engineers, Malaysia*, *75*(1).

Choi, C., Tolochko, O., & Kim, B. (2002), 'Preparation of iron nanoparticles by chemical vapor condensation,' *Materials Letters*, *56*(3).

Crisan, C. M., Mocan, T., Manolea, M., Lasca, L. I., Tăbăran, F. A., & Mocan, L. (2021), 'Review on Silver Nanoparticles as a Novel Class of Antibacterial Solutions,' *Applied Sciences*, *11*(3).

Danbature, W. L., Shehu, Z., Yoro, M., & Adam, M. M. (2020), 'Nanolarvicidal Effect of Green Synthesized Ag-Co Bimetallic Nanoparticles on <i>Culex quinquefasciatus; Mosquito,' *Advances in Biological Chemistry*, *10*(01).

Das, A. J., Kumar, R., & Goutam, S. P. (2016), 'Sunlight Irradiation Induced Synthesis of Silver Nanoparticles using Glycolipid Bio-surfactant and Exploring the Antibacterial Activity,' *Journal of Bioengineering & Biomedical Science*, *06*(05).

Davies, J., & Davies, D. (2010), 'Origins and Evolution of Antibiotic Resistance,' *Microbiology and Molecular Biology Reviews*, *74*(3).

Degu, A., Engidawork, E., & Shibeshi, W. (2016), 'Evaluation of the anti-diarrheal activity of the leaf extract of Croton macrostachyus Hocsht. ex Del. (Euphorbiaceae) in mice model,' *BMC Complementary and Alternative Medicine*, *16*(1).

Dikshit, P., Kumar, J., Das, A., Sadhu, S., Sharma, S., Singh, S., Gupta, P., & Kim, B. (2021), 'Green Synthesis of Metallic Nanoparticles: Applications and Limitations,' *Catalysts*, *11*(8).

Dikusar, A. I., Globa, P. G., Belevskii, S. S., & Sidel'nikova, S. P. (2009), 'On limiting rate of dimensional electrodeposition at meso- and nanomaterial manufacturing by template synthesis,' *Surface Engineering and Applied Electrochemistry*, *45*(3).

Dsouza, A., Shilpa, M. P., Gurumurthy, S. C., Nagaraja, B. S., Mundinamani, S., Ramam, K., Gedda, M., & Murari, M. S. (2021), 'CuAg and AuAg bimetallic nanoparticles for catalytic and heat transfer applications,' *Clean Technologies and Environmental Policy*, *23*(7).

Eltarahony, M., Zaki, S., ElKady, M., & Abd-El-Haleem, D. (2018), 'Biosynthesis, Characterization of Some Combined Nanoparticles, and its Biocide Potency against a Broad Spectrum of Pathogens,' *Journal of Nanomaterials*.

Farsi, M., & Farokhi, S. (2018), 'Biosynthesis of Antibacterial Silver Nanoparticles by Endophytic Fungus Nemania sp. Isolated From Taxus baccata L. (Iranian Yew),' *Zahedan Journal of Research in Medical Sciences, 20*(6).

FDA Guidance on Nanotechnology DOCUMENT: Guidance for Industry Considering Whether an FDA-Regulated Product Involves the Application of Nanotechnology. (2011), *Biotechnology Law Report, 30*(5).

Fernando, S., Gunasekara, T., & Holton, J. (2018), 'Antimicrobial Nanoparticles: applications and mechanisms of action,' *Sri Lankan Journal of Infectious Diseases, 8*(1).

Fredrick, O. O., & Mangaka, C. M. (2017), 'Electrochemical and optical band gaps of bimetallic silver-platinum varying metal ratios nanoparticles,' *African Journal of Pure and Applied Chemistry, 11*(1).

Gebrehiwota, H., Zelelewb, D., & Gebremariamc, H. (2018), 'Chemical analysis and medicinal activities of volatile components from the seeds of Croton macrostachyus plant', *International Journal of Sciences Basic and Applied Research, 37*(2).

Ghoreishi, S. M., Behpour, M., & Khayatkashani, M. (2011), 'Green synthesis of silver and gold nanoparticles using Rosa damascena and its primary application in electrochemistry,' *Physica E: Low-Dimensional Systems and Nanostructures, 44*(1).

Gulari, E., Güldür, I., Srivannavit, S., & Osuwan, S. (1999), 'Co oxidation by silver cobalt composite oxide,' *Applied Catalysis A: General, 182*(1).

Guo, Z., Chen, Y., Wang, Y., Jiang, H., & Wang, X. (2020), 'Advances and challenges in metallic nanomaterial synthesis and antibacterial applications,' *Journal of Materials Chemistry B, 8*(22).

Herlekar, M., Barve, S., & Kumar, R. (2014), 'Plant-Mediated Green Synthesis of Iron Nanoparticles,' *Journal of Nanoparticles*.

Hulkoti, N. I., & Taranath, T. (2014), 'Biosynthesis of nanoparticles using microbes—A review,' *Colloids and Surfaces B: Biointerfaces, 121*.

Huynh, K. H., Pham, X. H., Kim, J., Lee, S. H., Chang, H., Rho, W. Y., & Jun, B. H. (2020), 'Synthesis, Properties, and Biological Applications of Metallic Alloy Nanoparticles. *International Journal of Molecular Sciences*, *21*(14).

Iqbal, Z., Khan, M. S., Khattak, R., Iqbal, T., Zekker, I., Zahoor, M., Hetta, H. F., El-Saber Batiha, G., & Alshammari, E. M. (2021), 'Selective Oxidation of Cinnamyl Alcohol to Cinnamaldehyde over Functionalized Multi-Walled Carbon Nanotubes Supported Silver-Cobalt Nanoparticles,' *Catalysts*, *11*(7).

Iravani, S., Korbekandi, H., Mirmohammadi, S. V., & Mekanik, H. (2014), 'Plants in Nanoparticle Synthesis. *Reviews in Advanced Sciences and Engineering*, *3*(3).

Ismail, M., Khan, M., Khan, S. B., Khan, M. A., Akhtar, K., & Asiri, A. M. (2018), 'Green synthesis of plant supported Cu Ag and Cu Ni bimetallic nanoparticles in the reduction of nitrophenols and organic dyes for water treatment,' *Journal of Molecular Liquids*.

Jain, N., Bhargava, A., Majumdar, S., Tarafdar, J. C., & Panwar, J. (2011), 'Extracellular biosynthesis and characterization of silver nanoparticles using Aspergillus flavusNJP08: A mechanism perspective,' *Nanoscale*, *3*(2).

Jameel, M. S., Aziz, A. A., & Dheyab, M. A. (2020), 'Comparative analysis of platinum nanoparticles synthesized using sonochemical-assisted and conventional green methods,' *Nano-Structures & Nano-Objects*, *23*.

Jamkhande, P. G., Ghule, N. W., Bamer, A. H., & Kalaskar, M. G. (2019), 'Metal nanoparticles synthesis: An overview on methods of preparation, advantages and disadvantages, and applications,' *Journal of Drug Delivery Science and Technology*.

Janani, B., Alarjani, K. M., Raju, L. L., Thomas, A. M., Das, A., & Khan, S. S. (2020), 'A potent multifunctional Ag/Co-polyvinylpyrrolidone nanocomposite for enhanced detection of Cr(III) from environmental samples and its photocatalytic and antibacterial applications,' *Spectrochimica Acta Part A: Molecular and Biomolecular Spectroscopy*.

Jeevanandam, J., Barhoum, A., Chan, Y. S., Dufresne, A., & Danquah, M. K. (2018), 'Review on nanoparticles and nanostructured materials: history, sources, toxicity and regulations,' *Beilstein Journal of Nanotechnology*.

Jin, X., Mao, A., Ding, M., Ding, P., Zhang, T., Gu, X., Xiao, W., & Yuan, J. (2016), 'A Simple Route to Synthesize Cu@Ag Core–Shell Bimetallic Nanoparticles and Their Surface-Enhanced Raman Scattering Properties. *Applied Spectroscopy*, *70*(10).

Kainat, Khan, M. A., Ali, F., Faisal, S., Rizwan, M., Hussain, Z., Zaman, N., Afsheen, Z., Uddin, M. N., & Bibi, N. (2021), 'Exploring the therapeutic potential of Hibiscus rosa sinensis synthesized cobalt oxide (Co3O4-NPs) and magnesium oxide nanoparticles (MgO-NPs),' *Saudi Journal of Biological Sciences*, *28*(9).

Kajihara, K. (2013), 'Recent advances in sol–gel synthesis of monolithic silica and silica-based glasses,' *Journal of Asian Ceramic Societies*, *1*(2).

Kandpal, N. D., Sah, N., Loshali, R., Joshi, R., Prasad, J., Pandey, K., & Sharma, S. (2013), 'Studies on Ferrofluid Synthesized by Ultra-Sonication of Ferrite (Fe_3O_4) and Microwave Assisted Grating of Poly-Dimethyl Siloxane (PDMS) with Carboxylic Acids,' *Particulate Science and Technology*, *31*(5).

Khan, S. R., Naeem, A., Jamil, S., Islam Aqib, A., & Ashraf Janjua, M. R. S. (2019), 'Synthesis of manganese–tin oxide microparticles by the solvothermal method and study of application as a catalyst and additive,' *Environmental Technology*, *42*(8): pp. 1187–1195.

Kruis, F., Fissan, H., & Peled, A. (1998), 'Synthesis of nanoparticles in the gas phase for electronic, optical and magnetic applications—a review,' *Journal of Aerosol Science*, *29*(6).

Ksar, F., Ramos, L., Keita, B., Nadjo, L., Beaunier, P., & Remita, H. (2009), 'Bimetallic Palladium−Gold Nanostructures: Application in Ethanol Oxidation,' *Chemistry of Materials*, *21*(15).

Kuppusamy, P., Yusoff, M. M., Maniam, G. P., & Govindan, N. (2016), 'Biosynthesis of metallic nanoparticles using plant derivatives and their new avenues in pharmacological applications – An updated report,' *Saudi Pharmaceutical Journal*, *24*(4): pp. 473–484.

Langlois, C., Li, Z. L., Yuan, J., Alloyeau, D., Nelayah, J., Bochicchio, D., Ferrando, R., & Ricolleau, C. (2012), 'Transition from core–shell to Janus chemical configuration for bimetallic nanoparticles,' *Nanoscale*, *4*(11).

Larue, C., Castillo-Michel, H., Sobanska, S., Cécillon, L., Bureau, S., Barthès, V., Ouerdane, L., Carrière, M., & Sarret, G. (2014), 'Foliar exposure of the crop Lactuca sativa to silver nanoparticles: Evidence for internalization and changes in Ag speciation,' *Journal of Hazardous Materials*.

Lee, D. W., Tolochko, O. V., Turaev, F. R., Kim, D., & Kim, B. K. (2010), 'Synthesis and Characterization of WS₂ Nanoparticles by Chemical Vapor Condensation,' *Journal of Nanoscience and Nanotechnology*, *10*(1).

Letha, N., Ganesan, K., Nair, P. S. K., Azalewor, H. G., & Gani, S. B. (2016), 'Evaluation of in vitro antioxidant activity and phytochemical screening of Croton macrostachyus Hochst. by using different solvent extracts', *Am. J. PharmTech Res*.

Linh, D. H. T., Anh, N. P., Mi, T. T. A., Tinh, N. T., Cuong, H. T., Quynh, T. L., Van, N. T. T., Minh, N. V., & Tri, N. (2018), 'Biosynthesis, Characteristics and Antibacterial Activity of Silver Nanoparticles Using *Lemon Citrus Latifolia* Extract', *MATERIALS TRANSACTIONS*, *59*(9).

Magiorakos, A. P., Srinivasan, A., Carey, R., Carmeli, Y., Falagas, M., Giske, C., Harbarth, S., Hindler, J., Kahlmeter, G., Olsson-Liljequist, B., Paterson, D., Rice, L., Stelling, J., Struelens, M., Vatopoulos, A., Weber, J., & Monnet, D, (2012), 'Multidrug-resistant, extensively drug-resistant and pandrug-resistant bacteria: an international expert proposal for interim standard definitions for acquired resistance,' *Clinical Microbiology and Infection*, *18*(3).

Maiti, D., Tong, X., Mou, X., & Yang, K. (2019), 'Carbon-Based Nanomaterials for Biomedical Applications: A Recent Study,' *Frontiers in Pharmacology, 9*.

Makarov, V. V., Love, A. J., Sinitsyna, O. V., Makarova, S. S., Yaminsky, I. V., Taliansky, M. E., & Kalinina, N. O. (2014), 'Green" Nanotechnologies: Synthesis of Metal Nanoparticles Using Plants,' *Acta Naturae*, *6*(1).

Maroyi, A. (2017), 'Ethnopharmacological Uses, Phytochemistry, and Pharmacological Properties of *Croton macrostachyus* Hochst. Ex Delile: A Comprehensive Review,' *Evidence-Based Complementary and Alternative Medicine*.

Mashwani, Z. U. R., Khan, M. A., Khan, T., & Nadhman, A. (2016), 'Applications of plant terpenoids in the synthesis of colloidal silver nanoparticles,' *Advances in Colloid and Interface Science*.

Mehwish, H. M., Rajoka, M. S. R., Xiong, Y., Cai, H., Aadil, R. M., Mahmood, Q., He, Z., & Zhu, Q. (2021), 'Green synthesis of a silver nanoparticle using Moringa oleifera seed and its applications for antimicrobial and sun-light mediated photocatalytic water detoxification,' *Journal of Environmental Chemical Engineering*, *9*(4).

Meyers, M., Mishra, A., & Benson, D. (2006), 'Mechanical properties of nanocrystalline materials,' *Progress in Materials Science*, *51*(4).

Mohammadi, H., Nekobahr, E., Akhtari, J., Saeedi, M., Akbari, J., & Fathi, F. (2021), 'Synthesis and characterization of magnetite nanoparticles by co-precipitation method coated with biocompatible compounds and evaluation of in-vitro cytotoxicity,' *Toxicology Reports*.

Mohanapriya, S., Vennila, M., & Kowsalya, S. (2020), 'Synthesis and Characterization of ZnS Nanoparticles Using Co-precipitation Method,' *Asian Journal of Applied Chemistry Research*.

Mohd Yusof, H., Mohamad, R., Zaidan, U. H., & Abdul Rahman, N. A. (2019), 'Microbial synthesis of zinc oxide nanoparticles and their potential application as an antimicrobial agent and a feed supplement in animal industry: a review,' *Journal of Animal Science and Biotechnology*, *10*(1).

Murthy, H. C. A., Desalegn, T., Kassa, M., Abebe, B., & Assefa, T. (2020), 'Synthesis of Green Copper Nanoparticles Using Medicinal Plant *Hagenia abyssinica (Brace) JF. Gmel.* Leaf Extract: Antimicrobial Properties,' *Journal of Nano materials, pp.* 1–12.

Nanophysics and nanotechnology: an introduction to modern concepts in nanoscience. (2004), *Materials Today*, *7*(11).

Narayanan, K. B., & Sakthivel, N. (2011), 'Green synthesis of biogenic metal nanoparticles by terrestrial and aquatic phototrophic and heterotrophic eukaryotes and biocompatible agents,' *Advances in Colloid and Interface Science*, *169*(2).

Nelli, D., Krishnadas, A., Ferrando, R., & Minnai, C. (2020), 'One-Step Growth of Core–Shell (PtPd)@Pt and (PtPd)@Pd Nanoparticles in the Gas Phase,' *the Journal of Physical Chemistry C*, *124*(26).

Obey, J. K., von Wright, A., Orjala, J., Kauhanen, J., & Tikkanen-Kaukanen, C. (2016), 'Antimicrobial Activity of *Croton macrostachyus* Stem Bark Extracts against Several Human Pathogenic Bacteria,' *Journal of Pathogens*.

Ovais, M., Khalil, A. T., Islam, N. U., Ahmad, I., Ayaz, M., Saravanan, M., Shinwari, Z. K., & Mukherjee, S. (2018), 'Role of plant phytochemicals and microbial enzymes in biosynthesis of metallic nanoparticles,' *Applied Microbiology and Biotechnology*, *102*(16).

Padalia, H., Moteriya, P., & Chanda, S. (2015), 'Green synthesis of silver nanoparticles from marigold flower and its synergistic antimicrobial potential,' *Arabian Journal of Chemistry*, *8*(5).

Padilla-Cruz, A. L., Garza-Cervantes, J. A., Vasto-Anzaldo, X. G., García-Rivas, G., León-Buitimea, A., & Morones-Ramírez, J. R. (2021), 'Synthesis and design of Ag–Fe bimetallic nanoparticles as antimicrobial synergistic combination therapies against clinically relevant pathogens,' *Scientific Reports*, *11*(1).

Parang, Z., & Moghadamnia, D. (2019), 'Synthesis of Silver Nano-particles by Electrochemical Method and the Effects on the Serum Levels of Thyroid Hormones (T3, T4) in Adult Male Rats,' *Iranian Journal of Toxicology*, *13*(4).

Patil, n., bhaskar, r., vyavhare, v., dhadge, r., khaire, v., & patil, y. (2021), 'overview on methods of synthesis of nanoparticles,' *international journal of current pharmaceutical research*.

Pérez-Tijerina, E., Gracia Pinilla, M., Mejía-Rosales, S., Ortiz-Méndez, U., Torres, A., & José-Yacamán, M. (2008), 'Highly size-controlled synthesis of Au/Pd nanoparticles by inert-gas condensation,' *Faraday Discuss*.

Petcharoen, K., & Sirivat, A. (2012), 'Synthesis and characterization of magnetite nanoparticles via the chemical co-precipitation method,' *Materials Science and Engineering: B*, *177*(5).

Prasad Yadav, T., Manohar Yadav, R., & Pratap Singh, D. (2012), 'Mechanical Milling: a Top Down Approach for the Synthesis of Nanomaterials and Nanocomposites,' *Nanoscience and Nanotechnology*, *2*(3).

Prasankumar, T., Irthaza Aazem, V., Raghavan, P., Prem Ananth, K., Biradar, S., Ilangovan, R., & Jose, S. (2017), 'Microwave assisted synthesis of 3D network of Mn/Zn bimetallic oxide-high performance electrodes for supercapacitors,' *Journal of Alloys and Compounds*.

Prechtl, M. H., & Campbell, P. S. (2013), 'Metal oxide and bimetallic nanoparticles in ionic liquids: synthesis and application in multiphase catalysis,' *Nanotechnology Reviews*, *2*(5).

Raja, S., Ramesh, V., & Thivaharan, V. (2017), 'Green biosynthesis of silver nanoparticles using Calliandra haematocephala leaf extract, their antibacterial activity and hydrogen peroxide sensing capability,' *Arabian Journal of Chemistry*, *10*(2).

Rathi Sre, P., Reka, M., Poovazhagi, R., Arul Kumar, M., & Murugesan, K. (2015), 'Antibacterial and cytotoxic effect of biologically synthesized silver nanoparticles using aqueous root extract of Erythrina indica lam,' *Spectrochimica Acta Part A: Molecular and Biomolecular Spectroscopy*.

Riaz, M., Ismail, M., Ahmad, B., Zahid, N., Jabbour, G., Khan, M. S., Mutreja, V., Sareen, S., Rafiq, A., Faheem, M., Shah, M. M., Khan, M. I., Bukhari, S. A. I., & Park, J. (2020), 'Characterizations and analysis of the antioxidant, antimicrobial, and dye reduction ability of green synthesized silver nanoparticles,' *Green Processing and Synthesis*, *9*(1).

Sadeghi, B., & Gholamhoseinpoor, F. (2015), 'A study on the stability and green synthesis of silver nanoparticles using Ziziphora tenuior (Zt) extract at room temperature,' *Spectrochimica Acta Part A: Molecular and Biomolecular Spectroscopy*.

Sáez, V., & Mason, T. (2009), 'Sonoelectrochemical Synthesis of Nanoparticles,' *Molecules*, *14*(10).

Samuel, M. S., Selvarajan, E., Mathimani, T., Santhanam, N., Phuong, T. N., Brindhadevi, K., & Pugazhendhi, A. (2020), 'Green synthesis of cobalt-oxide nanoparticle using jumbo Muscadine (Vitis rotundifolia): Characterization and photo-catalytic activity of acid Blue-74,' *Journal of Photochemistry and Photobiology B: Biology*.

Seyedi, M., Haratian, S., & Khaki, J. V. (2015), 'Mechanochemical Synthesis of Fe_2O_3 Nanoparticles,' *Procedia Materials Science*.

Shafey, A. M. E. (2020), 'Green synthesis of metal and metal oxide nanoparticles from plant leaf extracts and their applications: A review,' *Green Processing and Synthesis*, *9*(1).

Shameli, K., Keshan Balavandy, S., & Abidin, Z. (2015), 'Green Synthesis of Silver Nanoparticles Using Sodium Alginate and Lignosulphonic Acid Blends,' *International Journal of electrochemical science*, *10*(1).

Sharma, A., Sagar, A., Rana, J., & Rani, R. (2022), 'Green synthesis of silver nanoparticles and its antibacterial activity using fungus Talaromyces purpureogenus isolated from Taxus baccata Linn,' *Micro and Nano Systems Letters*, *10*(1).

Sharma, G., Kumar, A., Sharma, S., Naushad, M., Prakash Dwivedi, R., ALOthman, Z. A., & Mola, G. T. (2019), 'Novel development of nanoparticles to bimetallic nanoparticles and their composites: A review,' *Journal of King Saud University - Science*, *31*(2).

Shrestha, S., & Adhikari, S. (2017), 'Size Dependent Optical Properties of Silver Nanoparticles Synthesized from Fruit Extract of Malus pumila,' *Journal of Nepal Chemical Society*.

Si, S., & Mandal, T. (2007), 'Tryptophan-Based Peptides to Synthesize Gold and Silver Nanoparticles: A Mechanistic and Kinetic Study,' *Chemistry - A European Journal*, *13*(11).

Simakin, A., Voronov, V., Kirichenko, N., & Shafeev, G. (2004). Nanoparticles produced by laser ablation of solids in liquid environment. *Applied Physics A*, *79*(4–6).

Singh, P., Kim, Y. J., Zhang, D., & Yang, D. C. (2016), 'Biological Synthesis of Nanoparticles from Plants and Microorganisms,' *Trends in Biotechnology*, *34*(7): pp. 588–599.

Singh, R., Shedbalkar, U. U., Wadhwani, S. A., & Chopade, B. A. (2015), 'Bacteriagenic silver nanoparticles: synthesis, mechanism, and applications,' *Applied Microbiology and Biotechnology*, *99*(11).

Singh, S., Gautam, R. K., Malik, K., & Verma, A. (2017), 'Ag-Co bimetallic catalyst for electrochemical reduction of CO 2 to value added products,' *Journal of CO2 Utilization*.

Sun, L., Yuan, G., Gao, L., Yang, J., Chhowalla, M., Gharahcheshmeh, M. H., Gleason, K. K., Choi, Y. S., Hong, B. H., & Liu, Z. (2021), 'Chemical vapour deposition,' *Nature Reviews Methods Primers*, *1*(1).

Swain, A. K. (2016), 'Review on Green Synthesis of Silver Nanoparticles by Physical, Chemical and Biological Methods,' *International Journal of Scientific & Engineering Research*, *7*(10).

Swihart, M. T. (2003), 'Vapor-phase synthesis of nanoparticles,' *Current Opinion in Colloid & Interface Science*, *8*(1).

Tavakoli, A., Sohrabi, M., & Kargari, A. (2007), 'A review of methods for synthesis of nanostructured metals with emphasis on iron compounds,' *Chemical Papers*, *61*(3).

Teshale A. Abeje. (2020), 'Phytochemical Investigation and Characterization on the Stem Bark Extract of Croton macrostachyus,' *Chemical and Process Engineering Research*.

Tsuzuki, T., & McCormick, P. G. (2004), 'Mechanochemical synthesis of nanoparticles,' *Journal of Materials Science, 39*(16/17).

Ullah, M., Ali, M., & Hamid, S. (2014), 'Structure-controlled Nanomaterial Synthesis using Surfactant-assisted Ball Milling- A Review,' *Current Nanoscience, 10*(3): pp. 344–354.

Veerasamy, R., Xin, T. Z., Gunasagaran, S., Xiang, T. F. W., Yang, E. F. C., Jeyakumar, N., & Dhanaraj, S. A. (2011), 'Biosynthesis of silver nanoparticles using mangosteen leaf extract and evaluation of their antimicrobial activities,' *Journal of Saudi Chemical Society*, *15*(2).

Vorokh, A. (2018), 'Scherrer formula: estimation of error in determining small nanoparticle size. *Nanosystems: Physics, Chemistry, Mathematics*.

Wakjira, K., & Negash, L. (2013), 'Germination responses of Croton macrostachyus (Euphorbiaceae) to various physico-chemical pretreatment conditions,' *South African Journal of Botany*.

Wang, L., Hu, C., & Shao, L. (2017), 'the antimicrobial activity of nanoparticles: present situation and prospects for the future,' *International Journal of Nanomedicine*.

Wang, Y., Zhao, H., & Zhao, G. (2015), 'Iron-copper bimetallic nanoparticles embedded within ordered mesoporous carbon as effective and stable heterogeneous Fenton catalyst for the degradation of organic contaminants,' *Applied Catalysis B: Environmental*.

World Health Organization (2014, April), '*Antimicrobial resistance: global report on surveillance,'* (No. 256). Dr Johan Struwe.

Wu, J., Bai, G. R., Eastman, J. A., Zhou, G., & Vasudevan, V. K. (2005), 'Synthesis of TiO_2 Nanoparticles Using Chemical Vapor Condensation,' *MRS Proceeding*

Yadav, R. N. S., & Agarwala, M. (2011), 'Phytochemical analysis of some medicinal plants,' *Journal of phytology*, *3*(12).

Yaqoob, A. A., Ahmad, H., Parveen, T., Ahmad, A., Oves, M., Ismail, I. M. I., Qari, H. A., Umar, K., & Mohamad Ibrahim, M. N. (2020), 'Recent Advances in Metal Decorated Nanomaterials and Their Various Biological Applications: A Review, '*Frontiers in Chemistry*.

Yuan, M., Liu, A., Zhao, M., Dong, W., Zhao, T., Wang, J., & Tang, W. (2014), 'Bimetallic PdCu nanoparticle decorated three-dimensional graphene hydrogel for non-enzymatic amperometric glucose sensor,' *Sensors and Actuators B: Chemical*, *190*: pp. 707–714.

Zhang, L., Zhou, L., Yang, K., Gao, D., Huang, C., Chen, Y., Zhang, F., Xiong, X., Li, L., & Xia, Q. (2016), 'Pd Ni nanoparticles supported on MIL-101 as high-performance catalysts for hydrogen generation from ammonia borane,' *Journal of Alloys and Compounds*.

Zhou, Y., Lin, W., Huang, J., Wang, W., Gao, Y., Lin, L., Li, Q., Lin, L., & Du, M. (2010), 'Biosynthesis of Gold Nanoparticles by Foliar Broths: Roles of Biocompounds and Other Attributes of the Extracts,' *Nanoscale Research Letters*, *5*(8).

Zhu, J., Gao, Q., & Chen, Z. (2008), 'Preparation of mesoporous copper cerium bimetal oxides with high performance for catalytic oxidation of carbon monoxide,' *Applied Catalysis B: Environmental*, *81*(3–4).